PETROLOGY

OF THE

CENTRE HILL COMPLEX

Centre Hill Mines

PETROLOGY OF THE CENTRE HILL COMPLEX, NORTHERN ONTARIO

By

NEIL D. MacRAE, B.Sc.

A Thesis

Submitted to the Faculty of Graduate Studies

in Partial Fulfilment of the Requirements

for the Degree

Master of Science

McMaster University

October 1963

MASTER OF SCIENCE (1963)
(Geology)

McMASTER UNIVERSITY
Hamilton, Ontario

TITLE: Petrology of the Centre Hill Complex, Northern Ontario

AUTHOR: Neil D. MacRae, B.Sc. (Queen's University)

SUPERVISORS: Dr. D. M. Shaw, Dr. T. N. Irvine

NUMBER OF PAGES: x, 102

SCOPE AND CONTENTS: Field relations of the banded mafic-ultramafic Centre Hill complex were studied and a single cross-section of the sill carefully mapped and sampled. Modal analyses were completed from thin sections of each specimen. Samples of all specimens were spectrographically analysed for nine elements: calcium, cobalt, chromium, copper, manganese, nickel, titanium, vanadium and zirconium. Thirteen samples, representing the major bands of the complex, were chemically analysed for the major oxides. Mineral composition variations were determined either by x-ray or optical methods and the trends plotted on a variation diagram. The criteria of classification and the magma differentiation trend were examined and discussed.

ABSTRACT

Field relations of the Centre Hill complex, one portion of a sill in the Abitibi Peridotite Belt, were studied and the best exposed cross-section of the sill carefully mapped and sampled. The general banded appearance, rhythmic layering, igneous lamination and proportion of mafic to ultramafic rocks suggest a stratiform type classification and in situ differentiation of a basaltic magma.

Modal analyses were completed for each specimen and these together with determined mineral composition variation were plotted on a variation diagram. Data from spectrochemical analyses for calcium, cobalt, chromium, copper, manganese, nickel, titanium, vanadium and zirconium for all specimens and major chemical analyses for thirteen of the principal bands were similarly plotted. The mineralogical and chemical trends support the suggested stratiform classification.

For the purpose of calculating successive magmas, band widths have been assumed to be proportional to volume. The normative composition of the calculated primary magma falls within the olivine tholeiite field of Yoder and Tilley's basalt classification.

The mechanisms of differentiation and crystallization have been discussed and compared with those of other stratiform bodies. To explain the noted reversals to more mafic products along the differentiation trend, periodic resurgence of basaltic magma into the chamber has been suggested.

ACKNOWLEDGEMENTS

This thesis was suggested by Dr. T. N. Irvine, previously of McMaster University. The work has been supervised by him and Professor D. M. Shaw, Chairman of the Department of Geology, McMaster University. Their combined surveillance has been most rewarding to the author. Valuable suggestions and criticism by Dr. H. P. Schwarcz, Dr. J. H. Crocket and other members of the Department of Geology were much appreciated. Many specimens, maps and field notes kindly were made available by Dr. J. Satterly of the Ontario Department of Mines. Mr. P. F. Hoffman prepared several of the included photomicrographs, and Miss M. Sounik, Mr. R. R. Keays and Mr. J. G. Payne assisted in coloring maps. Thanks is extended to Centre Hill Mines for permission to examine their property. Financial support for the project came through the Department of Geology, McMaster University.

TABLE OF CONTENTS

LIST OF ILLUSTRATIONS

INTRODUCTION

The Centre Hill complex is one of several mafic to ultramafic sills in Munro Township, District of Cochrane, Ontario. These sills compose a part of the 80-mile-long Abitibi Peridotite Belt which extends from Reaume Township at the northwest end to Holloway Township at the southeast end (Plate 1).

In 1944, under the direction of Dr. J. Satterly, a small part of Munro Township was mapped by the Ontario Department of Mines, the work being completed in 1950 (Satterly, 1951). Detailed mapping and sampling over one section of the Centre Hill complex by the author and Dr. T. N. Irvine of the Geological Survey of Canada during the latter part of September 1962, indicated only very minor modification to Satterly's map of that body.

F. C. Taylor, Satterly's chief assistant for the Munro project during 1950, later completed a Ph.D. thesis concerning the petrology of the mafic to ultramafic sills in the Matheson area (Taylor, 1955). He considered the ultramafic and gabbroic rocks to have originated from two distinct liquids, the material being intruded in two separate periods as a crystal mush. However, field evidence observed by Irvine and the author at the Centre Hill body seemed to support a theory of origin by differentiation from a single liquid. It was decided to test this hypothesis by carefully documenting one well-sampled cross-section of the sill.

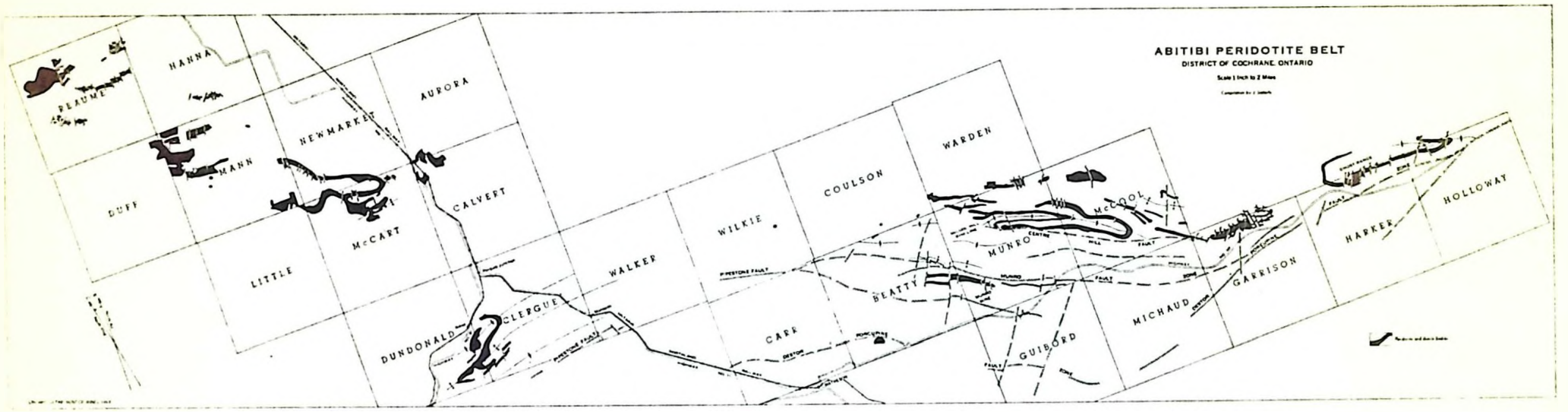

Plate 1: Abitibi Peridotite Belt. Reduced from Ontario Department of Mines map. Scale 1" = 7.7 miles.

GENERAL GEOLOGY

A complete picture of the geology of Munro Township is available from Satterly's 1951 report. A brief summary of the data pertaining to the Centre Hill area will suffice here.

A Table of Formations, as established by Satterly, is as follows:

Cenozoic	
Recent	Wind-blown sand (dunes), stream deposits, peat
Pleistocene	Sand, gravel, boulders; boulder clay; varved clay, silt; wind-blown sand (dunes)
	Great Unconformity
Precambrian	
Keweenawan (?)	Quartz diabase
	Intrusive Contact
Matachewan (?)	Quartz diabase, diabase
	Intrusive Contact
Algoman (?)	Quartz diorite, feldspar porphyry, felsite, lamprophyre
	Intrusive Contact
Basic and Ultrabasic Intrusives	Diorite, diabase, gabbro, peridotite and dunite (serpentinized), pyroxenite
	Intrusive Contact
Volcanics	Rhyolite, rhyolite agglomerate and tuff
	Andesite, basalt; pillow lava, diabase lava, spherulitic lava, fragmental lava (flow breccia), talc-chlorite schist, carbonate-chlorite schist; actinolitized and chloritized lavas
	Faulted Contact
Sediments	Greywacke, argillite, arkose, conglomerate

The sediments, thought to be the oldest rocks in the area, are mainly well-banded or fine-grained greywackes. They are limited to the extreme southwest corner of the township, separated from volcanics by the Contact Fault (Plate 2).

The volcanics, consisting of spherulitic basaltic flows, basic to intermediate pillow lavas with good flow breccia tops, and lenticular acidic volcanic bands, are divided into two general belts. The southern one between Contact and Munro faults is approximately 7000 feet wide, and the northern belt between Munro Fault and Centre Creek is approximately 9500 feet wide. From Centre Creek northward the succession becomes more complex, the country rock being mainly basalt, with some interbanded acidic lavas all conformably intruded by sheets of mafic to ultramafic rocks. Because of the association of sills with acid volcanic horizons Satterly has suggested that these rhyolite agglomerates and tuffs indicate favourably weak horizons for the later intrusions.

The oldest intrusive rocks in the area are Haileyburian type ultramafic and mafic sill-like bodies, discontinuous and lenticular along strike. The composition of some individual sills ranges from dunite through peridotite, pyroxenite and gabbro to diabase. Others are apparently wholly ultramafic or wholly gabbroic.

One small mass of Algoman quartz diorite spottily outcrops immediately southeast of Centre Hill.

Matachewan diabase dikes intrude the older rocks along a general north-south pattern.

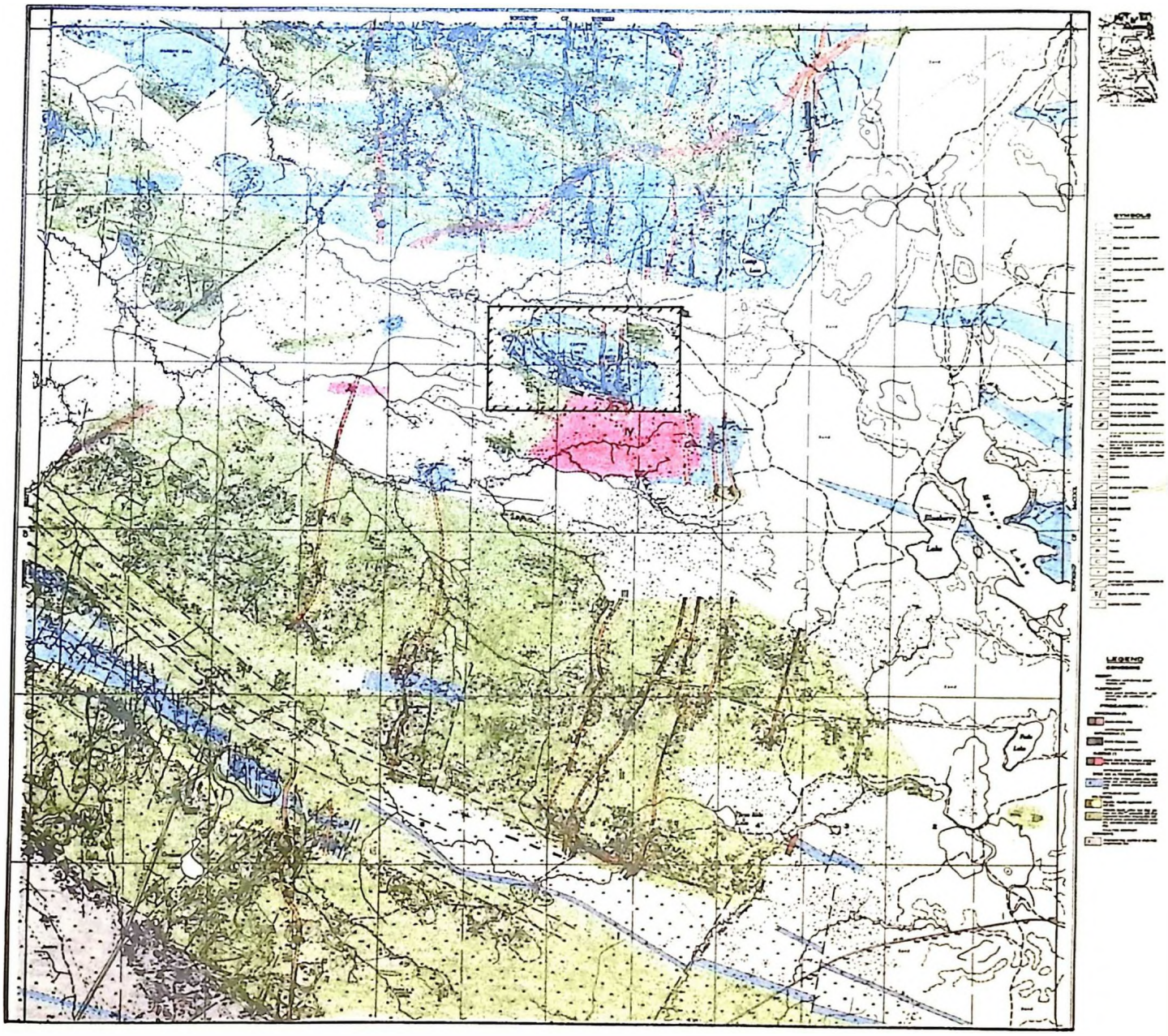

Plate 2: Geological Map of Munro Township, showing location of Centre Hill complex. Reduced from Ontario Department of Mines map. Scale 1" = 5,000'.

STRUCTURAL GEOLOGY

Numerous top determinations were possible in the lavas because of the well preserved pillows. Also, much helpful data come from the geophysical surveys and diamond-drilling programs carried out by various companies in the area.

In the southern part of the Township, the Contact and Munro faults trend approximately N60°W with undetermined movement. Between Contact Fault and Centre Creek most volcanic rocks dip south-southwesterly. Thus a major synclinal axis has been assumed through the Centre Creek area, with minor ripples to the north and south.

The nearly vertically dipping Centre Hill complex is sharply drag folded against the Centre Hill strike fault, which marks the southern side of the hill. There has been some breakage across the drag.

On the basis of the available geological and geophysical data, Satterly has postulated that the Centre Hill complex may be a part of a much larger sill which has been folded and faulted in a complicated form, stretching from southwestern Warden Township, through Munro Township and halfway through McCool Township (Plate 1).

METAMORPHISM

Regional metamorphism of the basic volcanic flows is of the greenschist facies, the common assemblage being actinolite-epidote-carbonate. Some fault zones show alteration to talc-chlorite schist and chlorite-carbonate schist. Actinolitization is most pronounced in the strike fault zones, as is the somewhat later carbonatization. Locally, both actinolitization and carbonatization may extend into the oldest diabase sills. Carbonatization and sericitization of Algoman and older

rocks is assumed by Satterly to be due to the action of hydrothermal solutions associated with the Algoman magma source.

In the ultramafic sills serpentinization and a later uralitization are the main metamorphic effects. In both the western dunite exposure and the peridotites of the main sill at Centre Hill serpentinization has taken place along fractures. A general decrease in serpentinization intensity is noted from base to interior of the sill. In thin sections of the ultramafic rocks small patches of talc can be found in the more highly altered shear zones. Magnesian carbonate minerals, as reject products of serpentinization, are not found in large amount in the Centre Hill area, although within several other sills of the belt talc-carbonate (magnesite) alteration products are extensive.

ECONOMIC GEOLOGY

Copper and gold accounted for all pre-1948 exploration in Munro Township and continue to be important. All sulphide deposits are located peripherally to ultramafic and mafic sills. On the north side of Centre Hill, Centre Hill Mines Ltd. have recently diamond-drilled approximately 30,000 feet and sunk an exploration shaft on a copper prospect. Most sulphide deposits of the area are very low in nickel content, reflecting, perhaps, an initially low nickel basic magma for the Haileyburian sills. Gold prospects are generally associated with quartz veins in basic lavas.

During 1948 Canadian Johns-Manville investigated an occurrence of asbestos, at what is now their Munro Mine, on the Munro Sill in Lots 10 and 11, Concession II. Munro Mine has been the sole continuous producer of asbestos in Ontario since 1950, when mill operations began. Much help in understanding the geology of the area has been gained from

the large amounts of data obtained by Canadian Johns-Manville and other companies who mapped and prospected the ultramafic sills.

ACCESS

The paved highway No. 101 extends eastward from Matheson, Ontario, through the southeastern end of Munro Township and on to connect with the Quebec highway network. Approximately 4 1/2 miles of good gravel and sand road leads north from the highway to the Centre Hill Mines site.

FIELD RELATIONS

Centre Hill is an elevated section of a generally east-west trending sill which has been drag-folded sharply against the southern major Centre Hill Fault (Plate 3). At the northern contact is a narrow band of rhyolite agglomerate which, on the west end, folds south and has a baked contact with a small serpentinized dunite plug. Several cross faults cut the sill at the crest of the drag-fold, but there is little displacement on them. The sill shows clear division into bands of different mineralogy, the bands dipping from 70 degrees northward to vertical. At the east end two north-south dikes of Matachewan diabase cut all other rocks and structures. The Centre Hill outcrop area is approximately 3600 feet long (east-west) and 1800 feet wide (north-south). A small plug of Algoman granite below the southeastern end of the sill, across Centre Hill Fault, has been indicated.

The location of the sample cross-section was chosen to show the best contact exposures. Each distinct or homogeneous band was called a 'unit', the measured width of each unit being assumed equal to its true thickness. Sample locations are noted on Plate 3.

The southern contact of the sill with metabasalt is sharp with the intrusive characteristics being a slight decrease in grain size of basalt toward the contact, a slightly baked and iron-stained appearance, and small tongues of ultramafic material into the basalt. The northern contact shows a decrease in grain size of gabbro toward the contact, recrystallization of adjacent rhyolite agglomerate illustrated by

development of feathery amphibole grains, and local iron staining and shearing.

Within the outcrop area of the sill contacts from band to band are commonly knife-sharp, with the exception of that between the upper feldspathic pyroxenite and gabbro, which is gradational over a few inches.

The sill may be broadly classified into four main divisions, the Basal Zone, the Ultramafic Zone, the Transition Zone, and the Gabbroic Zone.

The Basal Zone consists of poikilitic hornblende peridotite, distinctively reddish-brown on weathered surface and somewhat finer grained than the following peridotites. Very small serpentinized olivine grains are poikilitically enclosed by average 1/8 to 1/4 inch hornblende grains.

The Ultramafic Zone consists of interbanded grey-weathering poikilitic (pyroxene) peridotites and reddish-brown weathering pyroxenites. The pyroxenites are typically massive, medium- to fine-grained rocks which show an increase in interstitial feldspar and related alteration minerals northward in the sequence. Only one band, Unit No. 3 (Plate 3), contains a sufficient and consistent amount of olivine to be classed as olivine pyroxenite. The peridotites are all poikilitic in texture, the enclosing pyroxene grains being as large as one inch in diameter. The weathered surface is grey with the individual poikilitic grains in high relief (Figure 1). All fresh surfaces are black.

Locally, serpentinization along small fractures is evident (Figure 2), showing migrant secondary magnetite along the fracture surface and serpentine alteration inward. A few narrow picrolite and chrysotile veins are present in the more serpentinized areas.

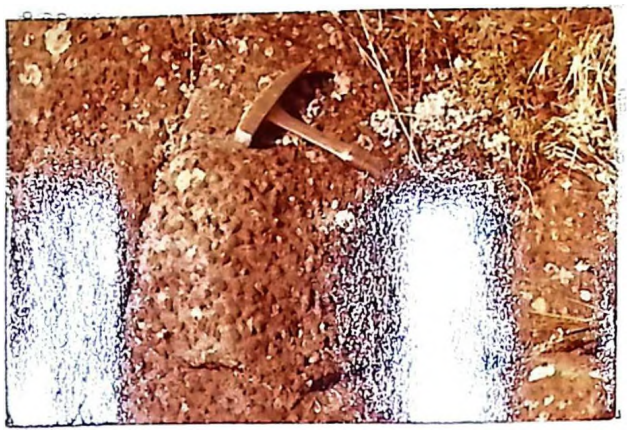

Figure 1. Weathered surface of poikilitic peridotite.

Figure 2. Serpentinization along fractures in poikilitic peridotite. Intersecting system of picrolite veins.

Layering is apparent in Unit 3, olivine pyroxenite (Figure 3), and in the peridotites (Figure 4). The layering - always parallel to band contacts - is, in both cases, compositional and mineralogical. Narrow olivine-rich and pyroxene-rich layers alternate rhythmically throughout the bands and any single layer is traceable along strike for many tens of feet.

Figure 3. Layering in olivine pyroxenite. Olivine pyroxenite lower left, poikilitic peridotite upper right.

Figure 4. Layering in poikilitic peridotite.

The Transition Zone consists of interbanded pyroxene-rich gabbro and normal gabbro. The first gabbro, Unit No. 14 (Plate 3), is interbanded over a narrow zone on the upper contact with pyroxene-rich gabbro (Figure 5). This narrow interbanding is continuous along strike from one end of the complex to the other. The gabbro layers of the Transition Zone show marked planar arrangement of feldspars parallel to the band contacts.

Figure 5. Interbanded pyroxene-rich gabbro and feldspar-rich gabbro.

The Gabbroic Zone is composed of massive, medium- to coarse-grained pyroxene and hornblende gabbros. Planar arrangement of minerals is absent although there is a distinct banding or layering effect caused by small-scale alternations of feldspar-rich and mafic-rich bands (Figure 6). Scattered bands of hornblende-bearing gabbros are common, but

Figure 6. Rhythmic layering in Gabbroic Zone.

typically these bands are discontinuous. Toward the north contact the grain size of the constituent minerals becomes much smaller.

Table I summarizes rock types, width of successive units and sample locations from the cross-section.

TABLE I. Sample Locations Within Each Rock Unit.

Unit No.	Rock Type	Layer Thickness	Footage From	Footage To	Sample No.	Sample Footage
1	Hornblende Peridotite	70 (ft)	0	70	24-7	2
					24-8	6
					24-9	15
					24-10	30
					24-11	69
2	Pyroxenite	90	70	160	24-12	72
					24-13	110
					24-14	157
3	Olivine Pyroxenite	30	160	190	24-15	161
					24-16	185
4	Peridotite	30	190	220	24-17	191
					24-18	210
					24-19	218
5	Pyroxenite	10	220	230	24-20	222
					24-21	229
6	Peridotite	70	230	300	24-22	231
					24-23	260
					24-24	295
7	Pyroxenite	55	300	355	24-25	303
					24-26	330
					24-27	351
8	Peridotite	30	355	385	24-28	357
					24-29	370
					24-30	384
9	Pyroxenite	119	385	504	24-31	388
					24-32	425
					24-33	500
10	Peridotite	3	504	507	24-34	505
11	Feldspathic Pyroxenite	30	507	537	24-35	515
					24-36	535
12	Peridotite	3	537	540	24-37	539
13	Feldspathic Pyroxenite	120	540	660	25-1	541
					25-2	600
14	Gabbro	95	660	755	25-3	670
					25-4	720
					25-5	745
15	Pyroxene-rich Gabbro	65	755	820	25-7	760
					25-8	810
16	Gabbro	670	820	1490	25-9	830
					25-10	930
					25-11	995
					25-12	1105
					25-13	1165
					25-14	1240
					25-15	1375
					25-16	1440
					25-17	1485

GENERAL MINERALOGY

Primary mineralogy of the Centre Hill complex is simple, the major minerals being olivine, clinopyroxene, calcic plagioclase, quartz and two amphiboles. Accessory minerals are ilmeno magnetite, apatite and very minor sulphides. Alteration, although severe in many cases, did not destroy completely the whole of the original grains and/or the essential textural features. Modal analyses were thus possible using primary minerals rather than secondary. Undoubtably discrepancies must occur between actual primary mineralogy and modal primary mineralogy. It is suspected, for example, that some secondary magnetite and quartz have been counted as primary. Similarly, where the reaction between plagioclase and pyroxene has resulted in a secondary chlorite-amphibole fibrous aggregate, the division of this aggregate between 'plagioclase' and 'pyroxene' is somewhat arbitrary.

For determining modal percentages each thin section was placed in a mechanical stage on a Leitz polarizing microscope and the tabulated individual mineral proportions of the first 800 point counts were converted to percentage figures.

Mineral composition variations were determined by either optical or x-ray methods.

A complete description of mineral characteristics is unnecessary here, thus only selective features are dealt with. Mineral associations and textures are considered in the section 'Microscopic Petrography'.

OLIVINE

Olivine composition determinations were made by B. Delabio, through T. N. Irvine, at the Geological Survey of Canada Laboratories in Ottawa. Unaltered olivine remnants were located in a thin section of the specimen, the section was then uncovered, the remnants flaked out with a sharp needle, and the powder mounted in a powder camera for x-ray exposure. Eight such determinations were made, the results of which, expressed as percentage forsterite, are shown in Table II.

TABLE II. Olivine X-Ray Determinations.

Sample No.	Spacing	Composition % Fo
24-10	141.80	77.5
24-11	141.80	77.5
24-16	141.55	74.5
24-25	141.36	72.5
24-30	141.57	75.0
24-31	141.12	69.5
24-34	140.73	64.3
24-37	140.70	64.0

Invariably, olivines or olivine pseudomorphs occur as rounded grains. Alteration is mainly to mesh-texture chrysotile with secondary magnetite and chlorite.

CLINOPYROXENE

Clinopyroxene occurs in two main forms; firstly, settled crystals, euhedral to subhedral in outline, are the major components of the pyroxenite units. Secondly, ophitic to poikilitic grains form the interstitial material of peridotites and gabbros. Alteration is mainly to dark green amphibole-chlorite fibrous aggregates, as a result of reaction with

plagioclase, or to tremolite. In zones of severe serpentinization of some peridotites, minor bastite serpentine is an alteration product.

Composition variation can be estimated from pyroxenite and gabbro samples only, the peridotite being too badly altered to obtain enough suitable fragments for the optical method used. Partial mineral separates in the case of gabbros and whole rock samples in the case of pyroxenites were used. Fragments of approximately 150 mesh size were sprinkled on a glass slide and immersed in oils for which the indices had been previously calibrated using an Abbe Refractometer. A temperature cell was not used, but a thermometer was kept near the microscope stage during the operation and corrections for deviations from 25°C made for each determination.

The method of orientation of mineral fragments such that Ny may be found is outlined by Hess (1960). Either {100} or {001} parting fragments may be used since both will show slightly off-center optic axis interference figures. Ny is aligned north-south by orienting the isogyre of the interference figure east-west. Ny may then be determined in sodium light.

In addition to the index of refraction of pyroxene, the optic angle must also be known to distinguish the composition. In uncovered thin sections, mineral grains showing yellow-grey interference colors and symmetrical extinction (i.e. grains showing acute bisectrix figures) were circled with india ink. After replacing the coverslip over an immersion oil, standard universal stage techniques were used to obtain 2V values. These optic angles were then corrected by means of the Fedorow chart (Emmons, 1943). Individual compositions are listed in Table III.

TABLE III. Pyroxene Determinations (Average of 3 Per Sample).

Sample No.	Ny	Corrected 2V	Composition
24-13	1.678	53°	Wo 50 En 44 Fs 06
24-15	1.677	50	Wo 52 En 42 Fs 06
24-21	1.681	51	Wo 49 En 42 Fs 09
24-26	1.681	50	Wo 49 En 41 Fs 10
24-32	1.682	50	Wo 49 En 40 Fs 11
24-36	1.679	54	Wo 49 En 45 Fs 06
25-1	1.686	50 1/2	Wo 45 En 40 Fs 13
25-8	1.697	48	Wo 38 En 40 Fs 22
25-10	1.700	48	Wo 37 En 37 Fs 26
25-16	1.699	45 1/2	Wo 36 En 38 Fs 26

The composition trend is shown in Figure 7 and compared with the Skaergaard pyroxene trend (Brown, Vincent 1963).

PLAGIOCLASE

Plagioclase, or its alteration products, in the Ultramafic Zone occupies an interstitial position. In the Gabbroic Zone it occurs mainly as euhedral to subhedral lath crystals but also as interprecipitate material, sometimes in association with quartz in micrographic texture. Alterations have been to saussurite and, where in contact with pyroxene, to finely fibrous amphibole-chlorite aggregates.

Composition variation was determined simply by estimating anorthite percentage with the aid of standard extinction curves (Kerr, 1959). In many cases alteration was too severe to allow any determinations, but for

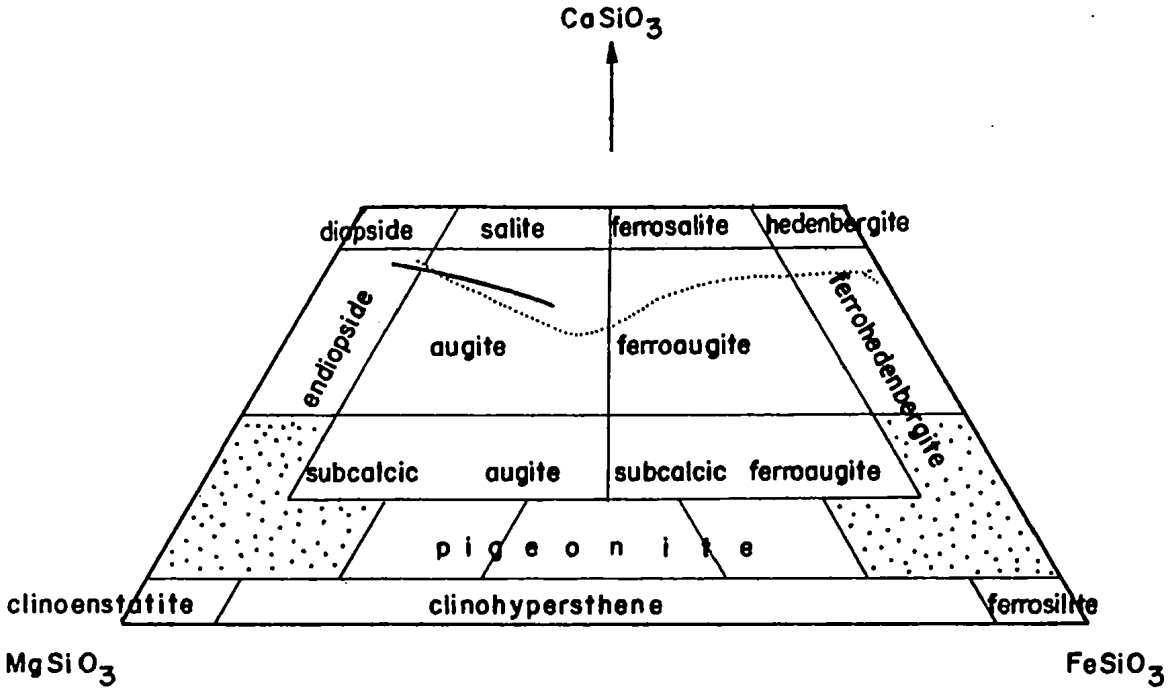

Figure 7. Clinopyroxene composition trend. Solid line - Centre Hill, dotted line - Skaergaard (Brown, Vincent 1963).

the less altered specimens general extinctions and cleavage show through the alteration products. Individual determinations are noted in Table IV.

TABLE IV. Plagioclase Determinations.

Sample No.	Composition % An
24-35	46
25-2	35
25-11	30
25-13	30
25-14	32
25-15	28
25-16	27

AMPHIBOLE

Two amphiboles occur in the Centre Hill cross-section. In the basal layer the major mineral component is a red-brown hornblende occupying an interstitial position. Briefly, the optical properties are as follows: large axial angle, negative optic sign, pleochroic with α very pale brown, β medium reddish brown and γ dark reddish brown, extinction $z \wedge C$ is approximately 15°, no twinning evident, and fairly good hornblende cleavage.

No mineral separation of this hornblende has yet been attempted, thus no chemical or x-ray analyses are now available.

Occurring more or less sporadically in the Gabbroic Zone are bands containing euhedral to subhedral pale green hornblende crystals.

OXIDES

Secondary magnetite is abundant throughout the Basal and Ultramafic Zones with much less in the Transition and Gabbroic Zones. Occurring as 'dust' within altered olivine or pyroxene crystals and as fracture and cleavage-filling material elsewhere, it tends to obscure the occurrences of primary opaques.

Primary ilmenomagnetite appears first in Unit 9 and generally becomes more abundant upward. The typical texture is skeletal magnetite with irregular forms of leucoxene. In several instances magnetite rods along octahedral planes form triangular shapes (Figure 8).

The ilmenite alterations may locally have migrated, leaving the interstices filled with secondary quartz, albite, amphibole or biotite.

Discrete grains of leucoxene are evidence in support of primarily precipitated ilmenite, in addition to the exsolved ilmenite from the ilmenomagnetite solid-solution.

SULPHIDES

No detailed study of the sulphides has yet been made, their occurrence being noted only in hand specimens and thin sections. They occur throughout the cross-section, but are most abundant in the Transition and Gabbroic Zones. Here, as in the Layered Series of the Skaergaard complex (Wager, Vincent, Smales 1957), they occur as small, discrete units in an interstitial position to the silicate grains.

In peripheral bodies of sulphides in the Centre Hill area copper is common but nickel is absent. It is probable that the primary liquid was low in nickel and, after the early-formed olivine and pyroxene grains had incorporated nickel in their structure, insufficient remained to form sulphides.

a

b

Figure 8. Skeletal magnetite showing exsolved structure.
a. Magnification x10, plane light.
b. Magnification x25, plane light.

MICROSCOPIC PETROGRAPHY

BASAL ZONE

The Basal Zone is in contact with a metabasalt. There is evidence of mobilization of iron and recrystallization at the contact. Thin section 24-06, cut from a specimen taken one foot within the metabasalts, shows small local amounts of olivine pseudomorphs poikilitically enclosed in a few patches of red-brown hornblende. This may be taken as evidence for the unevenness of the lower contact.

The Basal Zone is distinctive in that no pyroxene occurs here, its place being taken by a primary red-brown hornblende. Four thin sections of this zone were studied. A mineral-by-mineral analysis follows.

Olivine

The total estimated primary olivine in the lower section (24-07) is 5 percent while near the top of the zone (24-11) the amount increases to 30 percent. (Modal analyses are noted in Table VI.) Most of the primary olivine has now been completely altered to serpentine, magnetite and colorless amphibole (tentatively identified as tremolite-actinolite), but the grain outlines are commonly well preserved. Nowhere was sufficient fresh olivine available for optical study although from sections 24-10 and 24-11 enough could be picked out for powder x-ray analysis.

Not only is there a very apparent increase in total abundance of olivine from the basal contact inward, but also an increase in grain sizes, those in the lower section (average 0.05 mm) being generally less than one-quarter the average dimension in the upper section.

Olivines and olivine pseudomorphs occur as rounded grains poikilitically enclosed within an amphibole host. Those few areas of the thin section which show intense alteration with associated shearing give, naturally, the most unreliable modal counts for olivine. The larger olivines (and pseudomorphs) show a random fracture pattern, usually outlined by secondary magnetite resulting from the reaction

olivine ——→ serpentine + magnetite.

There is evidence of two periods of alteration in the olivine grains. The centers of the completely altered grains consist of serpentine with or without associated secondary magnetite. From the rims inward, in various degrees of growth, are fringes of colorless amphibole (tremolite ?) blades. Especially in the lower part of the Zone this tremolite alteration has completely replaced the serpentine in several grains. The extinction angle of the fringe tremolite seldom differs by more than 5 degrees from that of the immediately surrounding amphibole host.

Amphiboles

Two distinctly different amphibole minerals are the most abundant components of the Basal Zone; a primary red-brown hornblende occurs as remnants within its alteration product - light green actinolite.

The hornblende poikilitically encloses olivine grains, a texture typical of clinopyroxene of the more northern, or higher, peridotites (Figure 9). Its texture, color, size and alteration relationships are sufficient to assign the hornblende to a primary magmatic classification. There is no preferential concentration of magnetite at the contacts between primary hornblende and secondary actinolite, thus both are assumed

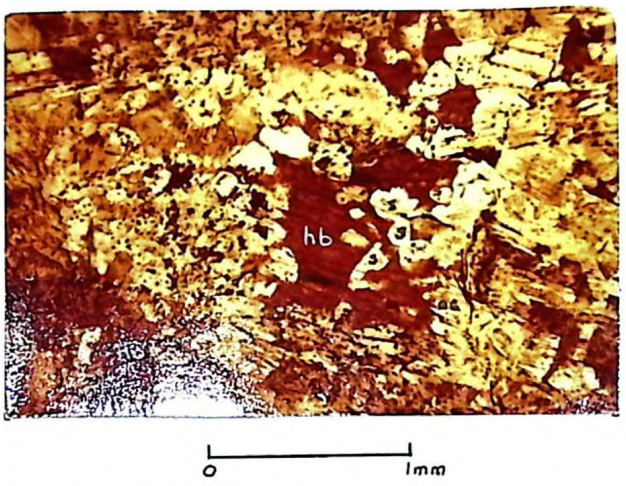

Figure 9. Basal hornblende peridotite, plane light.

to hold equivalent amounts of iron in their structure. It is impossible to estimate the size of the original hornblende grains except to note that they were probably larger than the present actinolite grains. Evidence for this is the occasional common extinction and pleochroism of hornblende remnants in adjacent actinolite grains. Commonly, the extinction angles of included hornblende and alteration actinolite differ by 3 or 4 degrees. This may be evidence of an incomplete structural adjustment of the hornblende lattice but with it still retaining compositional differences - as indicated by its distinctive color. Approximately 40 to 60 percent of the red-brown hornblende has been altered to actinolite.

The minerals of Figure 9 and following photomicrographs are labelled according to the symbols of Table V.

TABLE V. Legend for Photomicrographs.

actinolite	ac	micrographic intergrowth	mg
amphibole	am	olivine	ol
chlorite	ch	plagioclase	pl
clinopyroxene	cl	quartz	q
hornblende	hb	serpentine	s
magnetite	mt	tremolite	tr

Opaques

No sulphides or leucoxene are found in any of the thin sections, the only opaque being magnetite. Most magnetite here is secondary, commonly occurring as 'dust' within olivine pseudomorphs and locally outlining irregular grain edges, fractures and cleavage directions in the amphiboles.

An effort has been made, during all modal analyses, to differentiate between secondary and primary magnetite on the basis of shape. Those grains which show a somewhat rectangular form have been counted as 'primary'. It must be admitted that primary grains would act as nuclei for secondary magnetite and, in contrast, that any structural deformation of the rock would distort the primary grains. An argument to reduce the 'primary' amounts could be based on the fact that the secondary magnetite may also be rectangular in cross-section.

As expected from the equation

olivine ⟶ serpentine + magnetite

the amount of secondary magnetite rises sympathetically with olivine and olivine pseudomorphs.

Others

There is no texture or secondary mineral group that indicates the presence of primary orthopyroxene in the original rock. However, actinolitization is too severe to rule out this possibility.

Serpentine and chlorite both occur as secondary minerals, mainly pseudomorphous after olivine.

ULTRAMAFIC ZONE

Since field evidence suggests that the Centre Hill complex represents a section of a differentiated sill, it is expected that each successive layer or band will have certain unique petrographic features. For this reason details of each unit from each zone are presented sequentially.

Unit 2 (Pyroxenite)

Subhedral to euhedral primary settled clinopyroxene grains make up most of the rock. Narrow rims - additions to the settled grains from the original trapped pore-space liquid - are evident on many grains, but they have commonly altered to a pale green to clear amphibole (tremolite-actinolite). The primary grains also show alteration to amphibole, the extent of alteration increasing upward, or northward, through the unit (Figure 10).

A minor amount of red-brown hornblende occupies an interstitial position, but most of the interstitial material is an alteration product from a pyroxene-plagioclase reaction to give fibrous amphibole aggregates. No unaltered plagioclase remains although an estimated 6 to 10 percent was originally present.

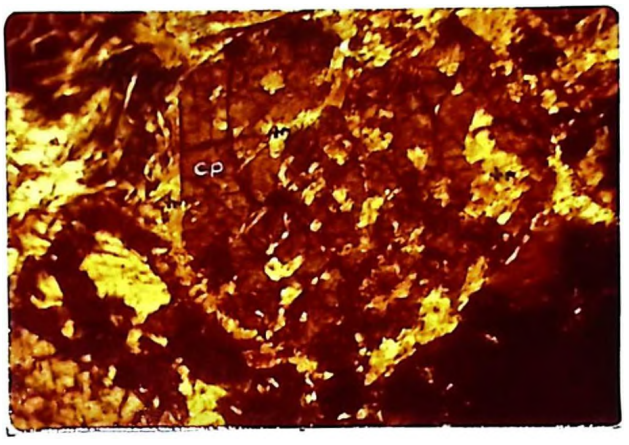

Figure 10. Settled clinopyroxene grain with growth rim, both showing alteration to amphibole (crossed nicols).

The only two opaque minerals are magnetite and leucoxene. Most of the magnetite appears to be primary, the remainder being alteration product of late metamorphism. The small amount of leucoxene is associated with amphibole-chlorite aggregates thus suggesting a breakdown of titaniferous pyroxene rather than ilmenite.

Toward the top of the band, in section 24-14, a number of discrete grains, averaging 1/16 to 1/8 inch in diameter, consist of fibrous amphibole, chlorite (penninite), carbonate, secondary magnetite and some leucoxene (Figure 11). The primary mineral which this distinctive assemblage represents can only be guessed at, but it is thought to be orthopyroxene. The only supporting evidences are the rectangular shape and the negative attribute that no similar alteration is found elsewhere in the cross-section.

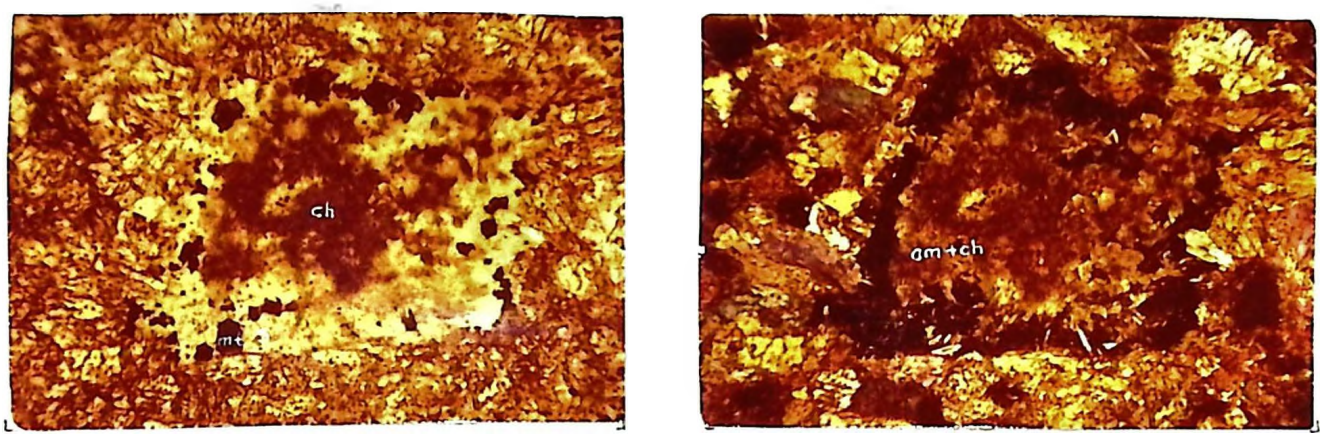

Figure 11. Altered orthopyroxene (?) grains.
a. Plane light.
b. Crossed nicols.

Unit 3 (Olivine Pyroxenite)

The amount of primary olivine varies from approximately 20 percent in section 24-15 (lower) to 50 percent in section 24-16 (upper). Evidence of shearing is abundant in the lower part of the unit where much secondary magnetite, chlorite and amphibole locally replace the primary minerals and obliterate primary texture. However, much of the upper primary mineralogy remains unaltered (Figure 12).

A decrease in the amount of settled clinopyroxene grains and a corresponding increase in the amount of interstitial clinopyroxene is evident from the base to the top. At the top, adjacent to a peridotite band, interstitial pyroxene becomes poikilitic in texture.

A minor amount of leucoxene, apparently as an alteration product of titaniferous pyroxene, is present.

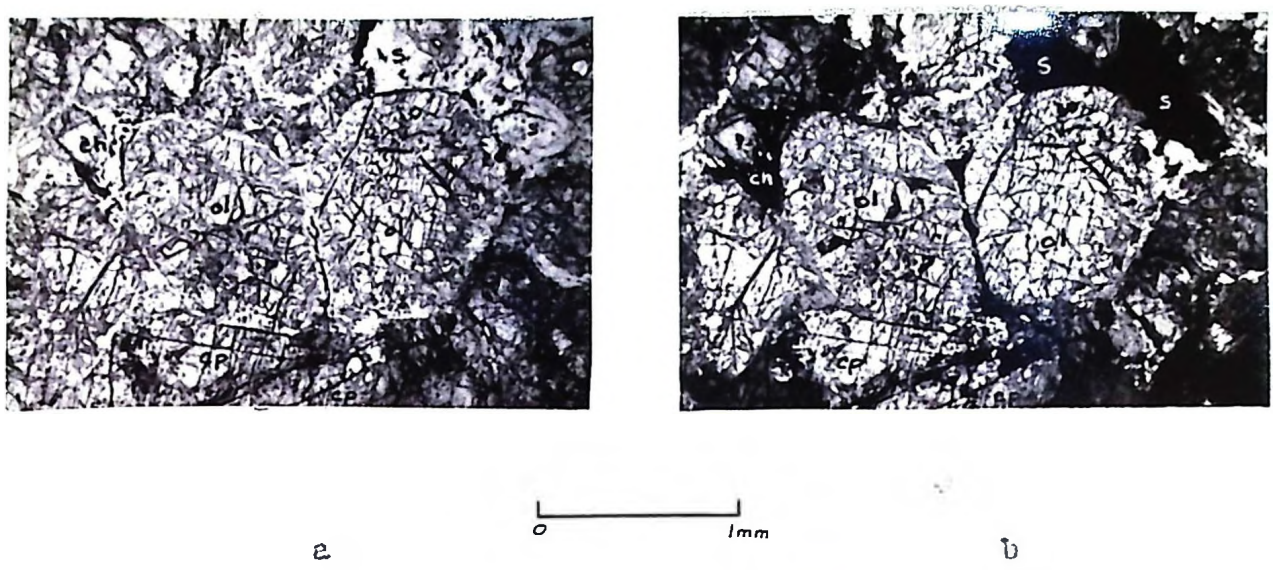

a b

Figure 12. Olivine pyroxenite.
a. Plane light.
b. Crossed nicols.

No trace of plagioclase or its common alteration form is found in the thin sections, but this may be due to the high degree of alteration in the unit.

Unit 4 (Peridotite)

The original rock consisted of primary settled, somewhat rounded, olivine grains enclosed by large grains of clinopyroxene with minor interstitial minerals. However, alteration has reached the point where no plagioclase or olivine and only scattered remnants of clinopyroxene remain. Tremolite is now the most abundant mineral as an alteration product of both clinopyroxene and olivine. Plagioclase and pyroxene have reacted to yield tremolite-chlorite aggregates and a reaction between olivine and pyroxene has yielded two chlorites (iddingsite and penninite) and magnetite.

Good evidence of tremolitization superimposed over serpentinization exists in section 24-17, where fibers of tremolite cut through serpentine flakes in olivine pseudomorphs.

In all three thin sections from this unit there is evidence of shearing becoming intense toward the top and resulting in brecciation of olivine grains. It is impossible to tell whether the disturbance took place before, during or after alteration of olivine. In the zones of greatest deformation a few scattered thread-wide chrysotile veinlets, rimmed by secondary magnetite, cut straight through the rock.

There is a general decrease in size of unbrecciated olivine grains upward in the unit.

Unit 5 (Pyroxenite)

Movement along the contact between Units 4 and 5 is responsible for obscuring much petrographic detail toward the top of Unit 4 and the bottom of Unit 5. Just as there is a decrease in olivine grain size toward the shear zone in Unit 4, there is an apparent increase in pyroxene grain size away from the zone in Unit 5. The explanation may simply be that the larger grains in the contact zone were brecciated and the smaller ones were not.

Because of the severe alteration at the lower contact, any estimate of the amount of interprecipitate plagioclase is uncertain, but must, in any case, be attempted. From the amount of dark green chlorite and amphibole aggregate typical of a reaction between pyroxene and plagioclase, it is estimated that plagioclase increases from 7 to 17 percent from bottom to top in Unit 5.

As is common to all pyroxenites in the cross-section, small rims on the settled grains have been added through a process of diffusion from trapped pore-space liquid. The simple twin plane (100) usually noted in the settled pyroxenites is not apparent on the rim material. Commonly, the rim material shows an earlier alteration to amphibole than the settled grains.

The grain size of the upper pyroxenes is distinctive in that it is so variable. Simply twinned, subhedral, small grains (average 0.17 mm) are interstitial to similarly twinned and shaped grains ten times their size.

Less magnetite and leucoxene are present in the thin sections of this unit than in the previous (lower) pyroxenites.

Unit 6 (Peridotite)

Unit 6 peridotite is similar to Unit 4 in that the major mineral constituents have been almost completely altered to tremolite, serpentine and chlorite with only the less altered patches showing primary texture. Olivine clearly shows two periods of alteration, the first being to serpentine and magnetite and the second to amphibole (tremolite). Chlorite also formed as a product of either stage. Those olivine pseudomorphs which are most completely tremolitized contain less secondary magnetite than the rest. The poikilitic clinopyroxene, of which few fresh remnants remain, has altered the tremolite, resulting in optically continuous tremolite fibers over each original grain for the included olivine pseudomorph and the host (Figure 13). The tremolite orientation over adjacent altered clinopyroxene grains usually varies. Secondary magnetite commonly outlines cleavage lines and cracks in the altered pyroxene.

In the most severely altered areas chlorite is abundant. Here, also, small shreds of biotite are frequently associated with magnetite.

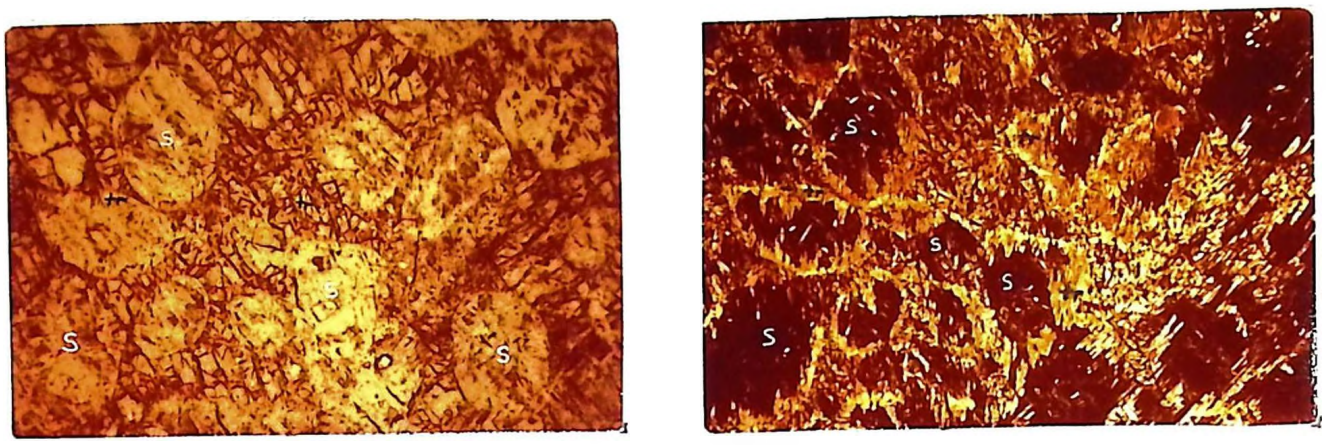

a. b.

Figure 13. Tremolitized poikilitic peridotite.
a. Plane light.
b. Crossed nicols.

Unit 7 (Pyroxenite)

Clinopyroxene is the major mineral throughout the unit, with minor and largely unaltered olivine grains in the lower part. Scattered primary magnetite and non-uniformly distributed interstitial altered plagioclase are minor minerals.

The clinopyroxene grains are generally subhedral due to narrow added rims, often are simply twinned and increase in grain size from bottom to top in the unit.

Alteration is not severe and shows a general decrease upward. Tremolite and light green pleochroic hornblende are the main secondary minerals after pyroxene, with light green amphibole-chlorite aggregates formed from reaction between pyroxene and interstitial plagioclase (Figure 14).

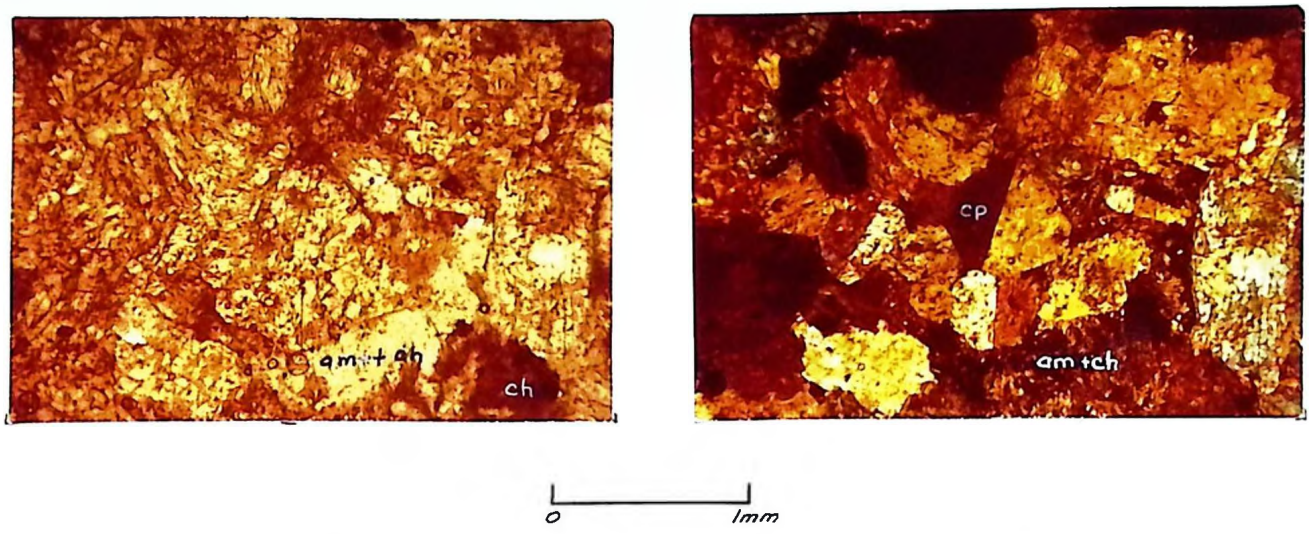

Figure 14. Slightly altered pyroxenite.
a. Plane light.
b. Crossed nicols.

In the upper part of the unit primary (?) magnetite has altered to limonite. A very minor amount of leucoxene is associated, suggesting the presence, originally, of small amounts of ilmenite.

Unit 3 (Peridotite)

Less severe alteration distinguishes this band from the previous peridotites. Only a few scattered olivine cores remain unaltered in the lower part (24-28), but in the upper part up to 30 percent of the section (24-30) is unaltered olivine. The host clinopyroxene is more completely altered, with fresh remnants only toward the top of the unit. There is heavy local separation of secondary magnetite, most being in interstitial position to the olivine pseudomorphs.

Near the base of the unit olivine grain size varies widely, but higher the percentage of small grains decreases and the larger ones increase in size.

A few chrysotite thread-veins are found in the lower part of the layer.

Unit 9 (Pyroxenite)

Matrix material is more abundant in this than previous pyroxenites, primary interstitial plagioclase starting at approximately 14 percent at the base and increasing upward to 26 percent. Complete alteration of the plagioclase to chlorite and amphibole and the appearance of light green hornblende after pyroxene gives the rock a distinctly greenish color.

Patches of talc occur along some shear zones and may be indicative of minor hydrothermal alteration.

The percentage of primary opaques is higher than for previous similar rocks due to the appearance of ilmenite. In the lower part of the unit no distinction between magnetite and ilmenite can be made in thin section, but at the top leucoxene replaces ilmenite. In the upper section (24-33) magnetite occurs in part as discrete grains but mainly as sharp 'ribs' within leucoxene. A few small grains of pyrite (?) were noted in section 24-32.

Units 10 and 12 (Peridotite)

These two three-foot wide units are sufficiently alike to warrent treatment under one heading. Both are badly altered poikilitic peridotites but contain approximately 20 percent fresh olivine remnants. However, between serpentinization-tremolitization processes and associated shearing, primary textures are obscured over much of the area of each thin section. Serpentine and chlorite (penninite and iddingsite) have developed abundantly about many of the olivine grains. Also, much secondary magnetite fills fractures and outlines numerous shear zones. Green to brown pleochroic hornblende with tremolite are the chief secondary products of clinopyroxene. Only occasional remnants of clinopyroxene can now be

found, occurring within the pleochroic hornblende which itself shows peripheral alteration to tremolite. Minor biotite shreds occur as partial rims to some magnetite grains. Traces of talc can be found in most shear zones. In both units sparse, narrow, magnetite-rimmed serpentine veins are found.

Unit 11 (Feldspathic Pyroxenite)

Little material from trapped pore-space fluid has been added to each settled clinopyroxene crystal in this unit, thus resulting in more nearly euhedral grains. Alteration of the pyroxene to medium to light green hornblende and tremolite peripherally and along fractures is not severe, but increases upward.

Plagioclase, only moderately altered, is the major interprecipitate constituent (Figure 15), amounting to a modal 28 percent at the top of

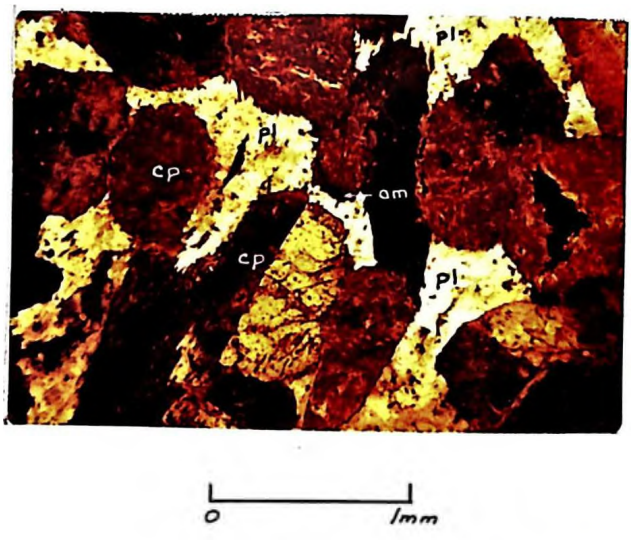

Figure 15. Interprecipitate plagioclase in pyroxenite; crossed nicols.

the unit. Much of the plagioclase is polysynthetically twinned. Alteration, which, as for pyroxene, increases slightly toward the top of the unit, is to amphibole, chlorite and zoisite. The fibrous amphibole is pleochroically medium to dark green and occurs (1) at plagioclase-

pyroxene contacts and (ii) in fractures within plagioclase where, apparently, mafic components have migrated.

Opaque material occurs in locally concentrated complex patterns. The material does not appear to be replacing any previous mineral or minerals, but simply occupies an interstitial position. In the lower section (24-35) leucoxene is the present opaque, apparently a reaction product of ilmenite and a Ca-component. Some magnetite 'ribs' within several leucoxene grains suggest that the primary mineral was ilmeno-magnetite. In the upper section alteration of the ilmenite, if it is present, has not taken place. No trace of sulphides was found in either section.

Scattered apatite needles appear within the interstitial feldspar.

Unit 13 (Feldspathic Pyroxenite)

Alteration is more severe in this unit than in the previous feldspathic pyroxenite. Plagioclase, which is interstitial to clino-pyroxene, is nearly completely altered to an aggregate of amphibole fibers and dense chlorite. Clinopyroxene shows varying degrees of alteration to pleochroic medium to dark green hornblende, with the average alteration being approximately 25 percent of any one grain.

Opaques, as in Unit 11, occupy an interstitial position and consist of leucoxene and magnetite in complex skeletal forms. However, in this unit there is some suggestion that the primary opaque, probably ilmeno-magnetite, locally replaced both pyroxene and feldspar as a late crystallizing phase. One large irregularly shaped grain of pyrite was noted in one section.

Toward the top of the unit (section 25-02) a trace of apatite, as needles within less altered plagioclase, was found.

TRANSITION ZONE

The Transition Zone consists of Unit 14, gabbro, and Unit 15, pyroxene-rich gabbro. As previously noted, these two units show an interbanded contact. This phenomenon is thought to result from interruption of the normal crystallization trend by contamination of the magma by injection of new liquid (see explanation in later section). Important petrographic features are noted in this zone, thus the units are treated separately here.

Unit 14 (Gabbro)

This unit marks the first occurrence of settled plagioclase crystals - previously all plagioclase occupied an interstitial position. The crystals occur as small but elongate laths which show a marked increase in planar arrangement upward in the band. Saussuritization has been complete, to the extent of partially obscuring the crystal boundaries. Presumably some of the trapped pore-space fluid crystallized to form interstitial plagioclase, but the settled laths are so small, numerous and altered as to prohibit estimation of amount of the interstitial phase. A significant trend in modal plagioclase percentage must be noted - from base to top the amount regularly decreases from approximately 75 percent to 47 percent.

At the base of the band clinopyroxene occurs as settled grains which have apparently acquired additional material from the pore-space fluid. The resulting grains tend to be ophitic. Toward the middle of the unit the pyroxene is completely ophitic, but again at the top it reverts to semi-ophitic texture. Alteration to light to medium green pleochroic hornblende is commonly nearly complete for the settled pyroxene and less so for the interstitial grains.

The opaques are somewhat different in occurrence from previous units. Pyrite, in semirounded shapes, increase in amount sharply toward the upper contact (although still less than 1 percent). At the base of the unit altered ilmenomagnetite in skeletal form is common. An increase in modal percentage from 3 and 2 percent respectively in the lower and and middle sections to 9 percent in the top section (25-05) is accompanied by a change in shape. The previous skeletal form is replaced by a smaller, more regular and sometimes rounded form. In reflected light, the previous steel blue-black color is replaced by a brownish black. Despite the color and form, this opaque is thought to be a partial alteration to oxide of magnetite rather than primary chromite (see Cr for 25-05, Table XII).

Only scattered occurrences of apatite needles within plagioclase can be found.

Unit 15 (Pyroxene-rich Gabbro)

The 1 1/2-foot interbanded lower contact consists of narrow (approximately 1 inch) hornblende gabbro bands in hornblende-pyroxene gabbro (Figure 5). In thin section, the contact between bands shows no physical break, only a mineralogical one. The settled hornblende crystals in the pyroxene-rich gabbro are apparently a carry-over from a hornblende gabbro reaction phase, since its modal percentage rapidly decreases upward from the contact zone.

Plagioclase is the major settled mineral of Unit 15, occurring as very elongate, narrow laths and maintaining an orientation preference. Saussuritization is slightly less than in the previous gabbro unit. Reaction with matrix material to form fibrous amphibole is, on the other hand, locally severe.

The only major primary interstitial constituent was apparently clinopyroxene, although few fresh remnants remain. Reaction has been to pleochroic light to medium green amphibole which commonly shows faint bluish tinges typical of sodic amphibole. Dense amphibole-chlorite aggregates have locally replaced both clinopyroxene and plagioclase, this amphibolitization hampering modal estimation of primary mineralogy.

Opaques in the contact zone at the base are idential to those of upper Unit 14. A gradual and incomplete change to skeletal form takes place away from the contact. No pyrite was noted in the sections.

Settled light to medium green, small hornblende grains and scattered settled clinopyroxene grains are found in the lower part of the unit. Apatite is an even more minor constituent, only a modal 'trace' being noted.

GABBROIC ZONE

The texture of this rock unit is completely different from that of the previous gabbros. Plagioclase and hornblende tend to be euhedral while pyroxene and quartz are anhedral. The resultant texture may be called intersertal (Moorhouse 1959). The rock is medium to locally coarse grained except near the top where a sharp decrease in grain size is noted.

The settled plagioclase crystals are generally subhedral, showing varying degrees of twinning, are locally normally zoned and are commonly saussuritized. Polysynthetic twinning is most abundant in the middle of the unit, the marginal sections showing more simple twinning. Clear evidence of normal compositional zoning exists in several sections, but alteration has made variation determinations impossible. Alteration of

the plagioclase laths has taken two forms; sericitization or saussuritization is relatively severe at the base and top of the unit and, for any zoned crystals, in the central zone. Amphibolitization, the second form of alteration, causes the edges of many crystals to appear ragged since it enters the crystals along most fractures. This fibrous amphibole is dark green, slightly pleochroic and developed as a reactant from plagioclase-pyroxene reaction (Figure 16).

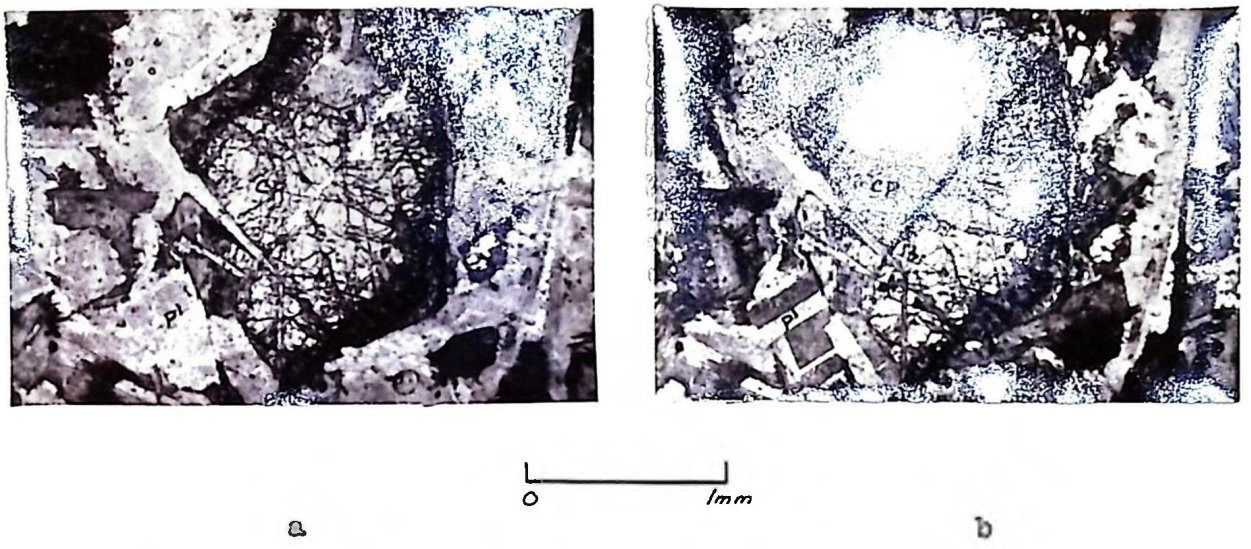

Figure 16. Secondary amphibole from pyroxene-plagioclase reaction.
a. Plane light.
b. Crossed nicols.

Hornblende, the second most abundant settled phase, is not evenly distributed through the Gabbroic Zone, but occurs in somewhat discontinuous bands, three of which were sampled. The crystals tend to have slightly ragged edges where alteration to fibrous amphibole is apparent, are usually simply twinned along their length, pleochroic light to medium green, smaller than associated plagioclase laths, and may locally have faint blue-green tinges to their edges.

The interstitial minerals are various forms of clinopyroxene, quartz and plagioclase. Clinopyroxene, the major component of this category, commonly is ophitic in texture (Figure 17), but only scattered

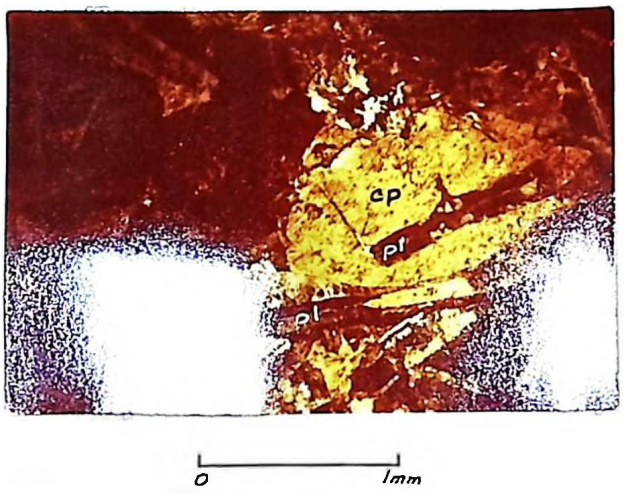

Figure 17. Ophitic clinopyroxene and long laths of plagioclase; crossed nicols.

remnants now remain. Alteration has been mainly to light green hornblende, but, where in contact with plagioclase, also to the previously described aggregates of amphibole and chlorite.

Micrographic intergrowth of plagioclase and quartz is present only in the lower half of the band (Figure 18), the initial modal percentage of 11 decreasing irregularly to 'trace' at the mid-unit point. The feldspar of the intergrowth is less saussuritized (thus less calcic) than the adjacent primary settled plagioclase crystals.

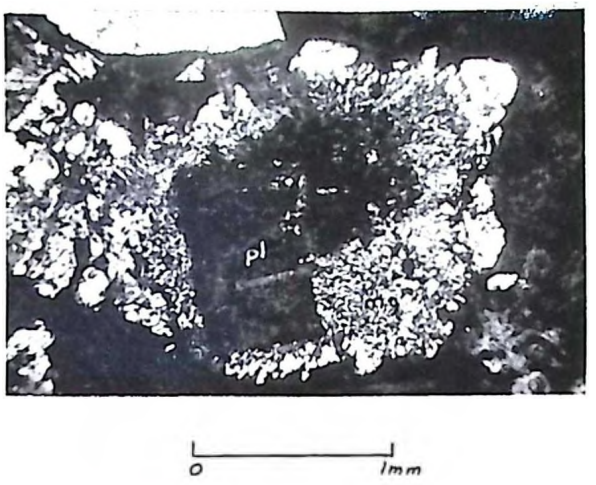

Figure 18. Graphitic quartz and plagioclase surrounding saussuritized plagioclase crystal; crossed nicols.

Quartz occurs as anhedral interstitial grains of varying size, commonly showing very slightly strained extinctions. Modal percents of quartz independent of graphitic quartz are shown in Table VI. A regular decrease from the initial 14.6 percent is apparent for the lower half of the unit with an increase in the upper half.

TABLE VI. Variation of Interstitial Quartz

Sample No.	Modal Quartz (%)
25-9	14.6
25-10	8.4
25-11	7.4
25-12	3.8
25-13	2.2
25-14	3.6
25-15	1.2
25-16	2.0
25-17	3.9

Pyrite occurs in small quantity but fairly consistently throughout the Gabbroic Zone as irregular, medium to large, anhedral and often semi-rounded grains.

The major opaque is ilmenomagnetite or its alteration products. The skeletal form previously noted for the same mineral in Units 9, 11 and 13 of the Ultramafic Zone reappears as the typical ilmenomagnetite form in the Gabbroic Zone. Although magnetite and ilmenomagnetite can produce skeletal forms as a settled phase, the grain relations here indicate a late interstitial phase. In some cases, intergrown plagioclase with common extinction over all included parts are found (Figure 19) and, rarely, pyroxene or pyroxene alteration products are partially included

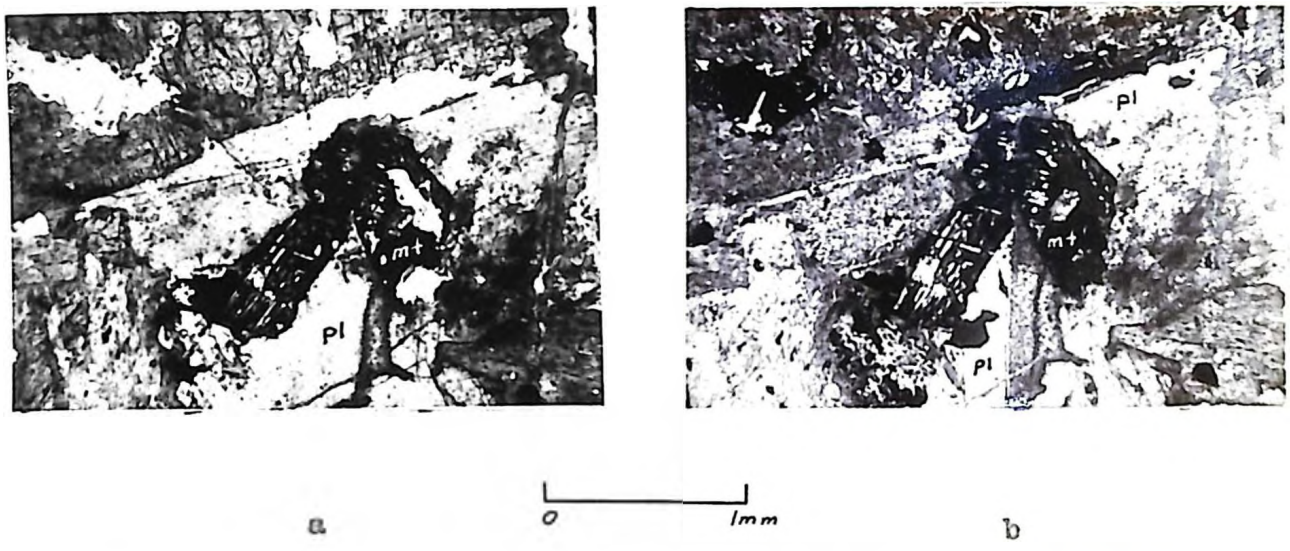

Figure 19. Skeletal magnetite intergrown with twinned plagioclase.
a. Plane light.
b. Crossed nicols.

in the opaque forms. Several of the opaques show skeletal magnetite ribs within slightly diffuse leucoxene grains (25-17). Exsolution of ilmenomagnetite and later alteration of ilmenite seems the logical explanation

of this texture. Locally, a partial rim of biotite on magnetite may be found.

Small apatite needles may be found through the Gabbroic Zone but are most abundant in the middle layers. Modal percentages for this mineral are probably inaccurate as the ease of identification varies directly with the severity of plagioclase alteration.

All gabbro thin sections were treated with hydrofluoric acid and sodium cobaltinitrate for the purpose of staining potash feldspar, but all results were negative.

MODAL ANALYSES

A complete list of primary mineralogy modal analyses and the derived mineral variation diagram are given in Table VII and are shown graphically in Figure 20.

TABLE VII. Modal Analyses. Mineral Abbreviations as in Table V.

Sample No.	Unit No.	ol	cl	orthopx	hb	opaques	pl	q	apatite
24-07	1	5.0			94.5	0.5			
24-08		20.0			79.0	1.0			
24-09		20.0			78.5	1.5			
24-10		30.0			69.0	1.0			
24-11		30.0			68.0	2.0			
24-12	2	3.6	85.4		-	3.0	8.0		
24-13			88.5		1.0	0.5	10.0		
24-14			86.5	(7.0)		0.5	6.0		
24-15	3	20.0	78.5			1.5			
24-16		49.3	50.2			0.5			
24-17	4	59.7	39.8			0.5			
24-18		58.0	41.5			0.5			
24-19		55.0	44.5			0.5			
24-20	5	1.0	90.0			2.0	7.0		
24-21			80.5			2.5	17.0		
24-22	6	58.0	41.5			0.5			
24-23		60.0	39.0			1.0			
24-24		60.0	39.0			1.0			
24-25	7	18.8	70.6			1.2	10.4		
24-26			87.5			0.5	12.0		
24-27			84.5			0.5	15.0		
24-28	8	61.0	34.0			5.0			
24-29		48.0	49.0			3.0			
24-30		50.0	48.0			2.0			
24-31	9	19.8	65.6			0.6	14.0		
24-32			75.7			2.3	22.0		
24-33			73.0			1.0	26.0		
24-34	10	49.8	49.4			1.0			
24-35	11		75.7			1.0	23.0		0.3
24-36			71.0			1.0	28.0		tr
24-37	12	49.8	49.2			1.0			
25-01	13		70.3			1.2	28.5		tr
25-02			73.8			1.4	24.8		tr
25-03	14		22.4			3.0	74.6		tr
25-04			43.9			2.3	53.8		tr
25-05			43.6			9.0	47.3		tr
25-07	15		72.3		1.2	4.5	22.0		tr
25-08			54.2		0.5	5.3	40.0		tr
25-09	16		19.8		7.2	4.4	48.7	19.9	tr
25-10			32.0		10.0	3.0	45.6	9.6	tr
25-11			39.4			2.6	49.4	7.6	1.0
25-12			32.4			5.0	55.6	5.9	
25-13			14.8		15.4	3.0	63.6	2.2	
25-14			28.0		0.8	3.8	63.3	3.6	
25-15			51.2			5.0	42.6	1.2	
25-16			45.0			4.5	48.5	2.0	
25-17			31.6		24.2	5.1	35.0	3.9	

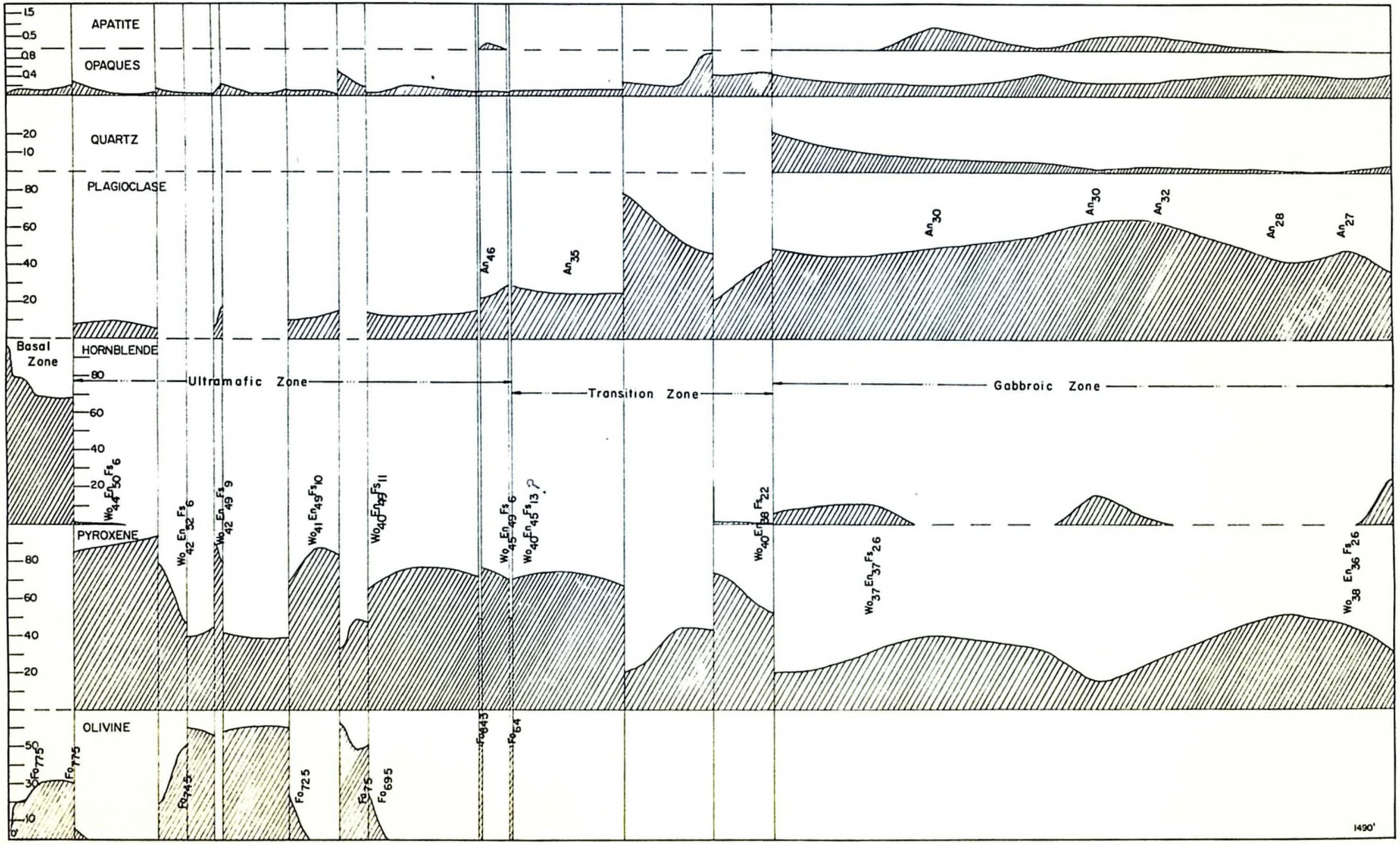

FIG 20 MINERAL VARIATION DIAGRAM

GEOCHEMISTRY

One procedure for primary sample preparation was used for both spectrochemical and wet chemical analyses. Approximately one-half of each hand specimen was crushed in a Bico-Braun steel jaw crusher, then ground to approximately -50 mesh in a ceramic disc pulverizer. The sample was then split to approximately 200 grams and final grinding to -150 mesh was done in a Spex Mixer Mill tungsten carbide vial. All sizing was done through steel sieves.

Owing to difficulty of mineral separation in highly altered rocks, only whole-rock analyses were made.

SPECTROCHEMISTRY

Eight minor elements and two major elements were analysed for by spectrographic methods, the procedural parameters of which are summarized in Table VIII. Line wavelengths and precision are noted in Table IX. Late in the process it was decided to omit all data concerning aluminum because of exceptionally poor precision and lack of correlation with values from the wet chemical analyses.

Of the specimens collected from the Centre Hill cross-section, a total of 52 (4 in metabasalts south of the intrusive, 47 within the intrusive, 1 in rhyolite agglomerate north of the intrusive) were analysed spectrographically.

TABLE VIII. Spectrograph Parameters.

Spectrograph	Jarrell-Ash 21-foot grating, Wadsworth mount, first order dispersion of 5.2 Å/mm
Condensing Optics	25 cm focal length cylindrical lens on horizontal axis at the slit; 6.7 cm focal length cylindrical lens on vertical axis at 16.1 cm from slit; 5 mm diaphragm at 27.5 cm from slit; 72.5 cm arc - slit distance
Arc Gap	4 mm
Slit Width	30 microns
Slit Length	11 mm
Intensity Control	7-step sector at slit, log intensity ratio 0.2, one wire-mesh screen
Electrodes	National Carbon Co. 'Special' grade 1/8" graphite rod cathode. United Carbon Products ultra-purity preformed 1/8" graphite electrode anode, 1/16" x 3/8" crater
Electrode Stand	ARL arc-spark stand, water-cooled jaws
Emulsions and Range	Eastman Kodak SA I plate, 2200-3500 Å; Eastman Kodak III-F plate, 3500-4800 Å
Processing	3 minutes in Kodak D19 developer at 20°C, 20 sec stop bath, 4 minutes acid fix, 1 hr water wash
Voltage	220 volts DC open circuit
Current	7 1/2 amps
Exposure	to completion; approximately 100 sec
Jet	Stallwood jet with 80% argon, 20% oxygen mixture at flow of 18 scfh. Silica glass cap over electrodes
Photometry	ARL photodensitometer, background corrections applied
Sample	1 part rock to 1 part graphite containing 0.033% Pd, 0.165% In
Artificial Standards	Prepared from Johnson-Matthey 'Spec pure' compounds. Matrix of 45% SiO_2, 40% MgO, 15% Fe_2O_3, mixed with sufficient oxides to give 50,000 ppm Ca, Al; 20,000 ppm Ti, Cr; 10,000 ppm Ni, Mn; 500 Ppm Co, V, Cu, Zr. Original plus 6 reductions cover a 100% to 3.2% range of primary mixture

TABLE IX. Line Wavelengths and Precision.

Spectral Line	Å	Precision C (%)
Al	2652.489	-
Ca	4425.44	4.4
Co	3453.505	7.1
Cr	3005.057	7.2
Cu	3273.962	10.6
Mn	4034.490	10.0
Ni	3003.629	7.0
Ni	3243.058	
Ti	4305.916	20.5
V	3183.406	7.3
Zr	3391.975	8.3
Pd	3242.703	-

Internal Standard

It was first decided to use Pd 3242 as internal standard line for all comparisons on Kodak SA I plates (2200-3500 Å) and In 4511 for all comparisons on Kodak III-F plates (3500-4800 Å). Later examination of the three high-range elements - calcium, manganese and titanium - plotted against both In 4511 and Pd 3242 showed satisfactory graphs in either case. Thus, especially for the sake of computation convenience, Pd 3242 was henceforth used for all comparisons.

Procedure

Samples of approximately 30 mg of the -150 mesh material previously prepared for each specimen were weighed on a torsion balance and each portion mixed in a one-to-one ratio with the graphite-palladium internal standard mixture. Mixing was done in small agate mortars. By wetting the sample with acetone during mixing only a five-minute period was required to assure uniformity. Three electrodes were filled from each sample portion and burned to completion under the conditions indicated in Table VIII.

Calculation

An Applied Research densitometer was used to read the percentage light transmission of the analysis and internal standard lines from the photographic plates.

The basic theory for obtaining element concentrations from transmission readings can be easily followed in such references as Ahrens and Taylor (1961) or Harvey (1950). Fundamentally, a curve, called a 'working curve', relating ppm to log I_A/I_E, where I_A is the corrected intensity of the analysis line and I_E is the corrected intensity of the internal standard line, is prepared using the artificial standards. Thus, once

a log I_A/I_E ratio is determined for any sample with an unknown concentration of the minor element, the concentration may be read from the previously prepared working curves for that element, provided that analysis parameters are constant in all cases.

An Intercom program prepared by D. M. Shaw for the Bendix G15D digital computer obtains log I_A/I_E determinations from transmission readings. Transmission readings from three successive steps for the analysis and internal standard lines together with a single reading of the 'background' transmission opposite the strongest of the three successive readings are required. From these data the computer program arranges for computation of a quadratic polynomial expressing the calibration of a narrow segment of the photographic plate, and the subsequent calculation of the corrected intensity ration, log I_A/I_E.

Working curves were prepared for all elements from the artificial standards, but it was later decided that for calcium a more realistic curve could be obtained using the values from the wet chemical analyses.

Precision and Accuracy

An analysis of variance procedure was used for each element from the results of triplicate analyses for each sample. The components of the sum of squares of deviation expression (see Ch. 10 Dixon and Massey 1957) were computed in logarithmic terms, on the Bendix computer and a pooled variance S_p^2 obtained. The antilog, g, of the deviation per determination ($S = S_p/\sqrt{3} = \log g$) is then calculated. For a given concentration, e.g. 10 ppm, there is a 66% probability that a repetition of the analysis will give a value between 10 g and 10/g. C, the precision value expressed as percent, is calculated as follows:

$$C\ (\%) = \frac{\text{upper limit - lower limit}}{2 \times \text{av. ppm}} \times 100.$$

Precision is reported in Table IX.

Since no ultrabasic standard is available for comparison analysis, an attempt was made to estimate accuracy by analysing W-1 (diabase standard). A comparison of the W-1 analyses averages and the recommended averages is given in Table X.

TABLE X. W-1 Spectrographic Comparisons. Recommended Averages from G.S.A. Bull. 1113.

	Average of 4 Analyses ppm	ppm (x 0.804)	Recommended Av. ppm
Co	77	62	51 (n.a.)
Cr	200	161	120
Cu	154	124	110
Mn	1915	1540	1340
Ni	102	82	82
Ti	8370	6740	7400
V	467	378	240
Zr	196	157	100

Without exception the W-1 values, using the working curves established for an ultramafic matrix, are high with respect to the recommended averages. Matrix effect is immediately suspected for at least a part of the deviation. A reduction by a factor of 0.804* of all analyses averages brings nickel to 82 ppm - the recommended value - and improves the correlation between the remainder. A reduction by such an

*log (W-1) - log (x) = q, where x is the obtained average ppm for nickel and q is the reduction factor.

arbitrary amount is perhaps not warrented in the absence of more concrete evidence, thus no alteration of the analyses has been made in future Tables or Figures.

A further indication of accuracy was obtained by comparing wet chemical values with spectrographic values for common samples. Calcium, manganese and titanium values were obtained with both methods, but only manganese and titanium may be compared since the wet chemical values were used as standards for the calcium working curve. The comparison is presented in Table XI.

Assuming both methods to be accurate, all points should lie on a straight line through the origin on a two-axis plot of spectrographic versus wet chemical values. Such graphs are presented in Figure 21. A reasonable linear correlation between methods exists for titanium but one of the methods for manganese determinations is apparently unreliable. J. Myssen reports a maximum 0.01% error in wet chemical MnO determinations (personal communication), thus the spectrographic method must be inaccurate.

Finally, four samples of basic to ultrabasic rocks from the Lac des Mille Lacs area, Ontario, previously analysed spectrographically by Watkinson (1963), were partially reanalysed. The comparison is reported in Table XII.

Many of the reported values are within the precision range but others, such as chromium and vanadium for I 60-85, differ markedly.

Improvement in method and control are needed in the spectrographic analysis of ultramafic samples. In future, no attempt should be made to

TABLE XI. Comparison of Spectrographic and Wet Chemical Analyses of Manganese and Titanium. Wet Chemical Values Recalculated to ppm Metal.

Sample No.	Spectrographic		Wet Chemical	
	Mn ppm	Ti ppm	Mn ppm	Ti ppm
24-08	1860	3270	1390	5250
24-10	1560	2810	1390	3670
24-13	2570	4150	1470	3900
24-18	1880	1270	1630	1570
24-23	1230	1100	1700	2020
24-26	1120	2550	1370	3370
24-28	1730	1020	2090	1650
24-33	1490	4010	1550	4940
24-35	2150	6130	1470	6150
25-08	2560	9830	1940	11400
25-12	3390	15060	1860	11000
25-15	2380	6000	1630	10570
25-17	2700	5740	1700	11400

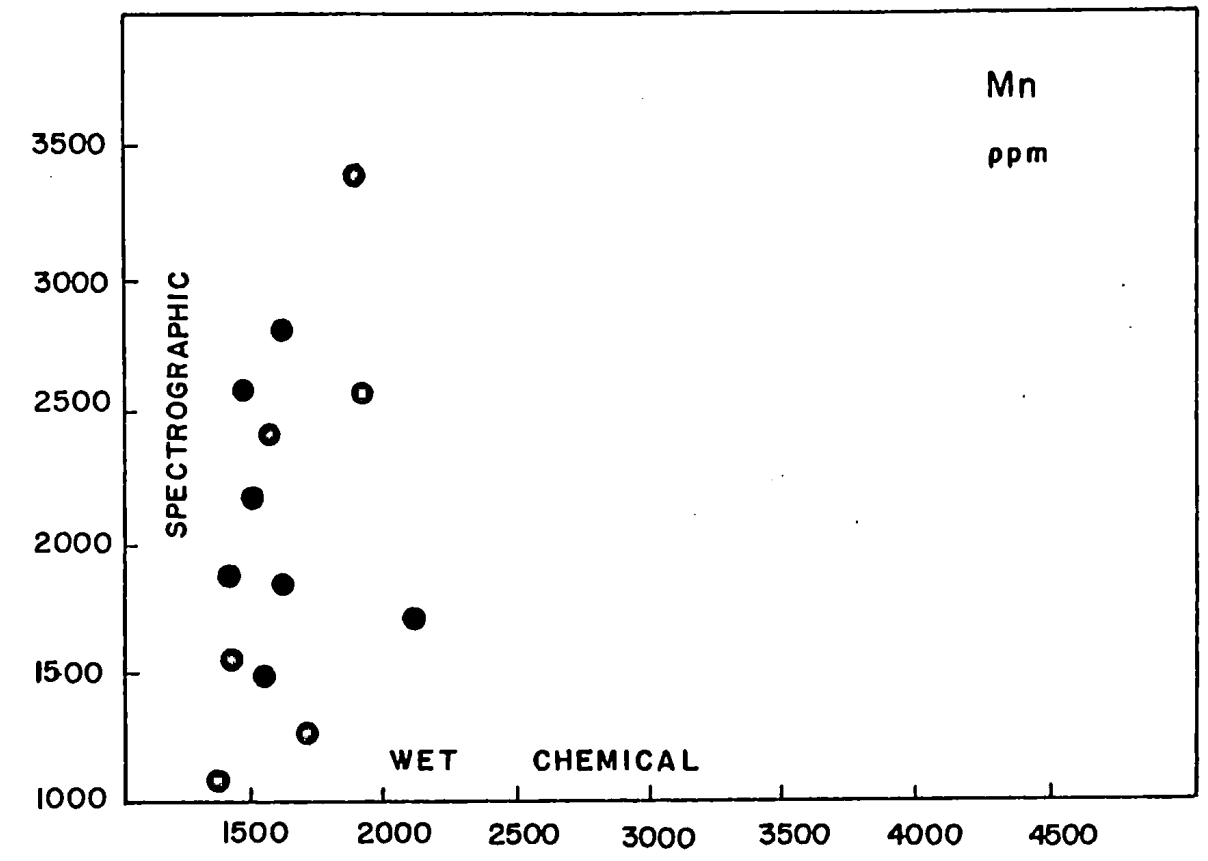

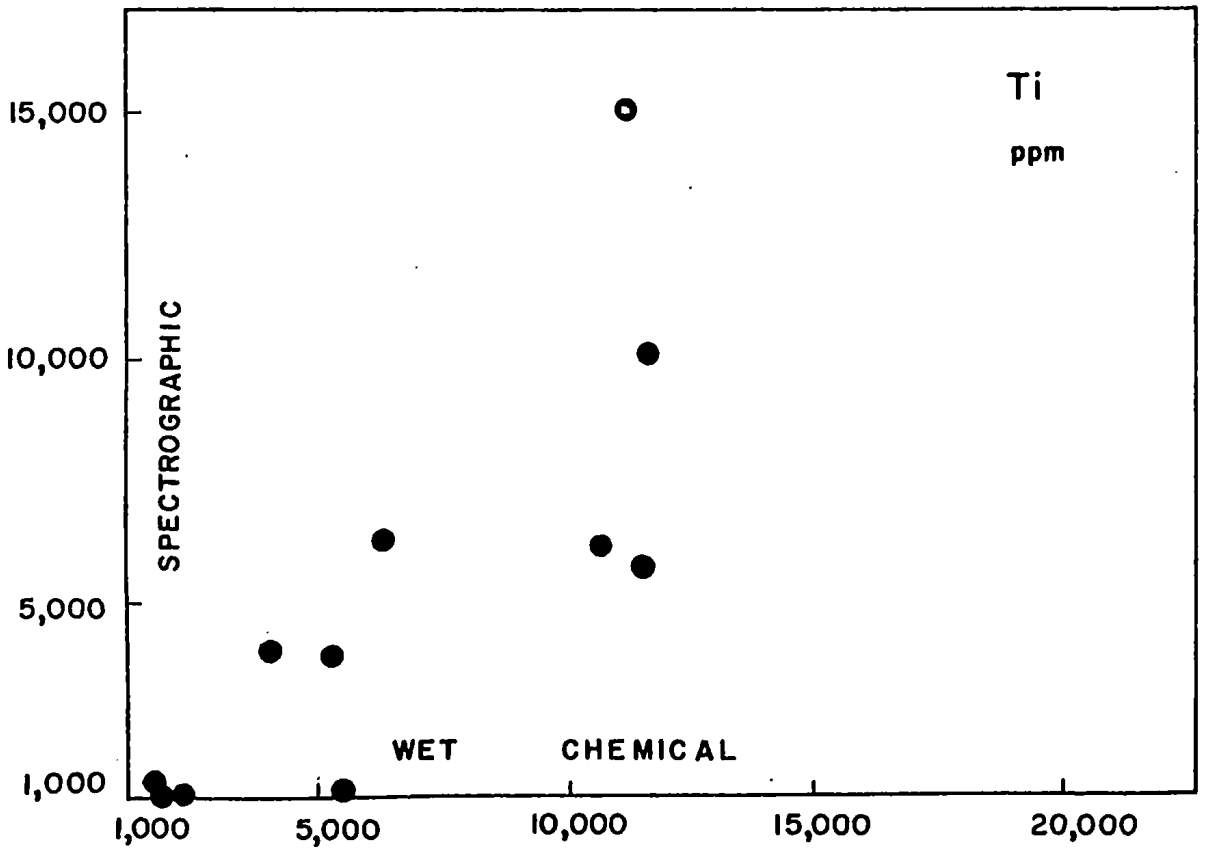

Figure 21. Correlation of spectrographic and chemical analyses of manganese and titanium.

TABLE XII. Comparison with Lac des Mille Lacs Samples; M - MacRae, W - Watkinson.

Sample No.	Mn		Ti		Cu		Co		Ni		Cr		Zr		V	
	M	W	M	W	M	W	M	W	M	W	M	W	M	W	M	W
I 60-85	1730	1000	5500	6700			101	43			587	1800	167	35	483	290
I 60-114	1290	970	7820	9200	65	57	90	70	318	360	1950	2050	85	46	523	470
W 60536					12	24	140	190	1260	1600	4920	4200			125	115
W 60543					42	20	200	130	1930	2100	7400	4700			81	43

vary major and minor elements within one standard - the effects on volatilization and arc temperature of large variation of Al_2O_3 and CaO are significant. The artificial standards composed of oxide mixtures burned more rapidly and more violently than the silicate samples, thus some attempt should be made to obtain several silicate standards. The matrix used to establish working curves for the whole range of concentration of each element was of ultramafic composition. Separate standards of mafic and ultramafic composition should have been used.

At this point, certain conclusions may be drawn:

1. Precision is probably good enough to compare ultramafics one with another.

2. Precision is probably good enough to compare mafics one with another.

3. There may be systematic errors in each group of rock analyses.

4. These systematic errors are probably different. Hence, quantitative comparisons can be made but one must be cautious comparing ultramafics and mafics.

Results

A complete list of average spectrographic analyses for each sample is tabulated in Table XIII. Figures 22a and 22b are variation diagrams of element concentration versus height in the cross-section.

MAJOR CHEMICAL CHEMISTRY

Thirteen samples representing major bands within the intrusion were analysed by wet chemical methods by J. Myrsson, Rock Analyst at McMaster University. Portions of the previously crushed material were set aside for this purpose.

TABLE XIII. Spectrographic Analyses for 9 Elements; Average of 3 Replicates for Each Sample.

Sample	Footage	Unit No.	Ca	Co	Cr	Cu	Mn	Ni	Ti	V	Zr
24-03	ctc -15	(basalt)	54600	76	660		1680	52	4300	169	128
24-04	ctc -8		57300	85	400	71	1840	63	4190	412	85
24-05	ctc -5		57700	96	650	75	1930	69	6590	314	100
24-06	ctc -1		67300	107	2380	123	2080	712	6770	247	118
24-07	2	1	51700	112	2360	23	1840	1060	5400	226	127
24-08	6		56600	115	5370	72	1860	1060	3270	306	84
24-09	15		50900	126	4020	31	1790	1200	4540	191	100
24-10	30		38200	120	5380	15	1560	1390	2810	195	57
24-11	69		28400	114	5020	14	2060	1350	3380	139	79
24-12	72	2	71300	77	3920	16	2310	520	4130	159	81
24-13	110		107200	111	2740	58	2570	408	4150	268	69
24-14	157		72400	90	1870	22	2180	417	3030	275	65
24-15	161	3	79000	121	960	19	2032	673	3280	181	53
24-16	185		47500	203	790	22	1600	1530	1820	111	63
24-17	191	4	30700	133	620	8	3920	1490	3170	72	80
24-18	210		22600	146	4670	14	1880	1280	1220	112	52
24-19	218		12400	186	9850	14	2640	1510	1560	99	56
24-20	222	5	110700	89	7920	44	2050	593	3200	198	50
24-21	229		77300	95	3430	18	1650	512	4280	153	93
24-22	231	6	31500	115	4560	29	3290	1740	2300	160	60
24-23	260		19900	165	4560	11	1230	1340	1100	95	46
24-24	295		24100	162	6150	27	3380	1810	2230	172	65
24-25	303	7	58800	112	2970	77	1553	738	3980	156	72
24-26	330		77200	71	2180	32	1120	386	2550	221	46
24-27	351		67700	139	9630	29	1170	327	2470	287	55
24-28	357	8	15700	172	5350	17	1730	1920	1020	208	45
24-29	370		20800	142	7170	58	2010	1540	1670	186	73
24-30	384		46300	185	6280	25	2290	2030	1940	175	10

TABLE XIII. Spectrographic Analyses for 9 Elements (Continued).

Sample	Footage	Unit No.	Ca	Co	Cr	Cu	Mn	Ni	Ti	V	Zr
24-31	388	9	63000	106	3110	78	1370	522	2060	208	60
24-32	425		112300	110	2670	57	2580	587	3840	272	67
24-33	500		90800	92	1010	11	1490	306	4010	428	62
24-34	505	10	24300	234	200	73	3320	1050	2820	140	119
24-35	515	11	118300	72	710	33	2150	177	6130	376	135
24-36	535		69700	86	1510	72	1330	280	3630	450	90
24-37	539	12	21400	232	200	256	5150	858	1750	78	105
25-01	541	13	65000	92	200	47	1380	233	3430	220	89
25-02	600		67300	99	200	289	1360	317	4020	410	93
25-03	670	14	83500	72	200	222	1270	52	5120	310	124
25-04	720		58200	88	1217	26	1090	58	3820	410	84
25-05	745		64200	115	200	428	1990	108	13230	1670	148
25-07	760	15	42400	129	200	381	2230	88	9070	693	157
25-08	810		62800	140	2170	620	2560	63	9830	973	117
25-09	830	16	41800	71	1800	14	1670	15	9500	74	254
25-10	930		62500	87	200	14	4560	5	15330	41	327
25-11	995		67000	123	200	26	4720	5	20000	49	413
25-12	1105		67300	86	2180	29	2810	62	13270	108	294
25-13	1165		75300	93	200	25	3390	56	15060	136	241
25-14	1240		54300	90	200	41	5340	38	13100	187	284
25-15	1375		61800	88	200	16	2380	53	6000	527	303
25-16	1440		47000	96	200	63	2760	65	6870	515	157
25-17	1485		43000	83	200	23	2700	57	5740	418	257
25-18	etc +3	(rhyolite)	48600	104	1660	124	2653	473	7200	260	168

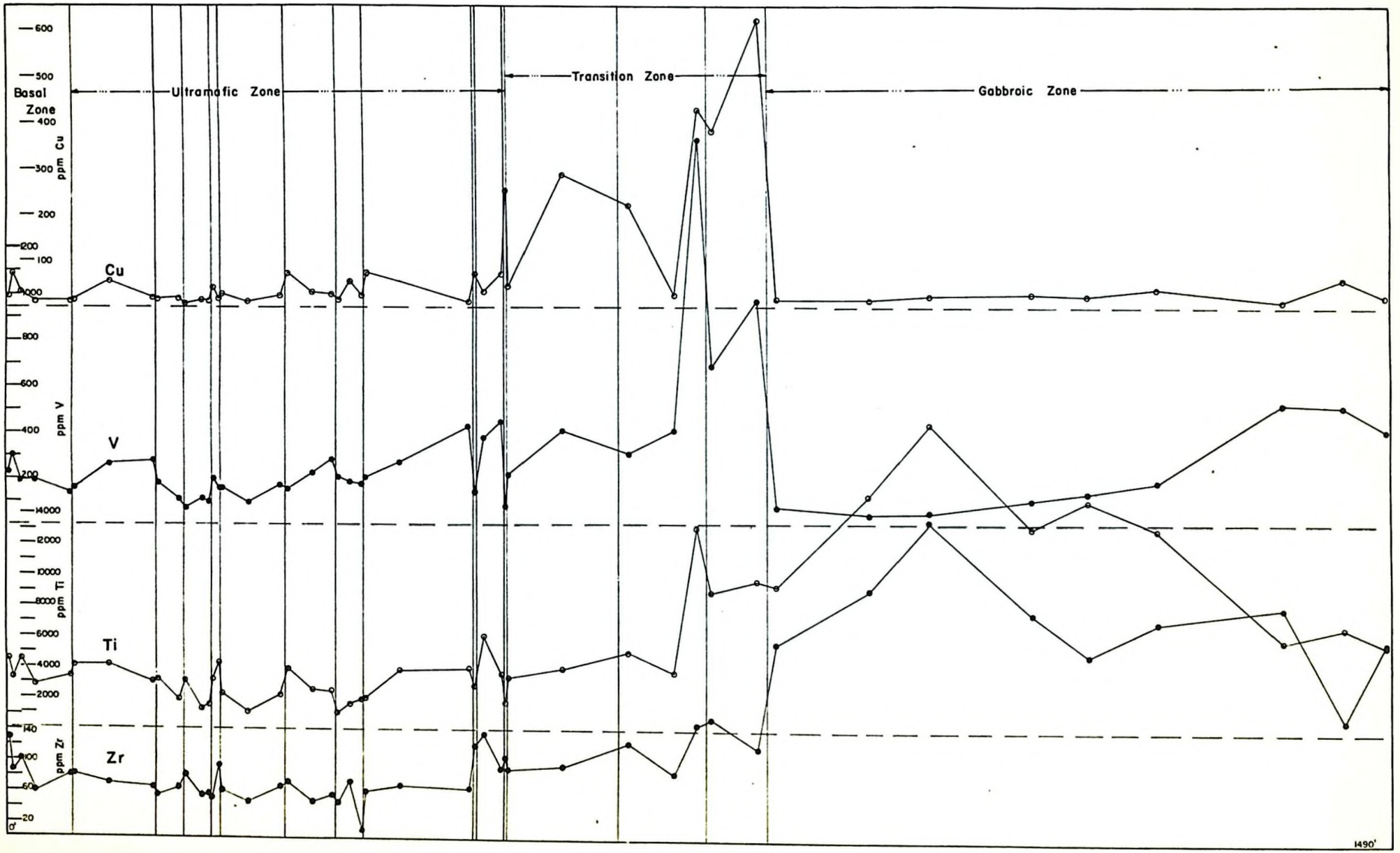

FIG 22a · ELEMENT VARIATION DIAGRAM

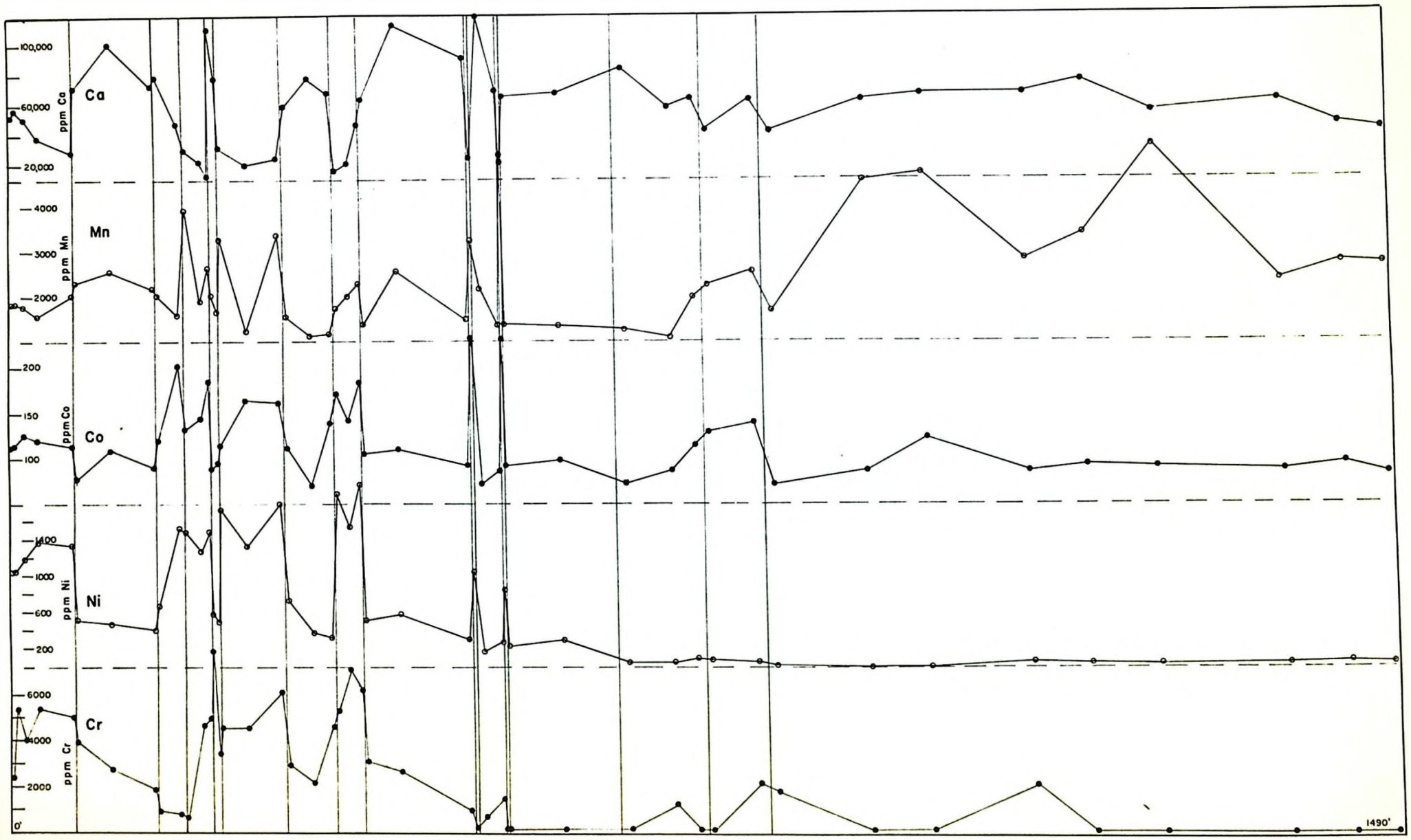

FIG 22b

ELEMENT VARIATION DIAGRAM

Results, reported as oxide percentages, are tabulated in Table XIV and variation with height illustrated in Figures 23a and 23b. In order to obtain a more complete picture of oxide variation, chemical compositions were calculated for those units which lacked wet chemical analyses. These calculations were based on modal analyses, making use of the determined mineral composition variations, and on spectrochemical analyses. A complete list of compositions, both analysed and calculated, is presented in the Appendix.

CORRELATION AND INTERPRETATION

Two major assumptions must be made prior to interpretation of data or comparisons to other similar intrusions. The first is that alteration of the primary mineralogy has been isochemical with respect to the elements considered and the second that the spectrographic determinations are comparable from sample to sample.

Two-element orthogonal plots for various pairs of elements were constructed and are shown in Plate 4. Several conclusions may be drawn from a brief examination of the diagrams. In the first place, a straight line relationship progressive from one rock group to another is most apparent for Ni-Cr and less so for Ni-Co and Ti-V. Secondly, the basal hornblende peridotite analyses invariably plot intermediate between pyroxenite and peridotite but closer to the latter group. Thirdly, one pyroxenite point usually lies within the peridotite group of points - this is the olivine pyroxenite of Unit 3.

More significant conclusions may be reached after a detailed study of the diagrams, while keeping in mind the limitations of the plots. Each point represents a whole-rock analysis, thus all minerals present will have a bearing on the location of the point. For peridotites, olivine and clino-

TABLE XIV. Major Element Analyses (Weight Percent)

	24-08	24-10	24-13	24-18	24-23	24-26	24-28	24-33	24-35	25-08	25-12	25-15	25-17
SiO_2	44.6	41.8	50.4	38.0	38.6	51.2	38.8	49.5	51.5	44.9	54.5	50.3	48.7*
TiO_2	.70	.49	.52	.21	.27	.45	.22	.66	.82	1.52	1.47	1.41	1.52
Al_2O_3	6.04	3.97	4.21	2.00	2.02	3.03	1.68	4.23	5.06	13.6	13.0	13.5	13.0
Fe_2O_3	3.71	6.78	1.49	10.7	10.8	1.34	11.0	1.52	.53	3.8	3.7	3.2	2.2
FeO	9.73	6.29	7.99	4.81	4.73	6.62	5.01	8.96	9.02	14.6	12.1	11.4	13.0
MnO	.18	.18	.19	.21	.22	.17	.27	.20	.19	.25	.24	.21	.22
MgO	20.6	27.0	16.0	30.8	30.1	17.1	30.2	14.9	12.9	7.1	2.0	5.0	6.5
CaO	7.92	5.50	16.3	2.87	3.27	18.2	1.97	16.6	16.3	17.7	5.9	8.2	6.8
Na_2O	.72	.52	.79	.05	.04	.39	.04	.63	1.65	2.29	5.14	4.28	3.32
K_2O	.10	.02	.03	.01	.01	.00	.03	.03	.10	.52	.23	.15	.37
P_2O_5	.05	.02	.01	.01	.02	.01	.02	.00	.04	.07	.21	.09	.11
H_2O^+	4.89	6.68	1.45	9.32	8.79	1.30	9.40	1.69	.95	3.00	1.38	2.26	3.51
H_2O^-	.13	.25	.17	.51	.51	.17	.56	.18	.16	.20	.20	.16	.26
CO_2	.05	.09	.15	.06	.06	.01	.04	.75	.34	.07	.13	.12	.62
Ign	5.09	6.99	1.9	10.0	9.41	1.8	9.74	2.83	1.9	3.7	1.96	2.84	4.47
Total	99.4	99.6	99.7	99.6	99.4	100.0	99.2	99.9	99.6	99.6	100.2	100.3	100.1
Rock-type	hb.-perid.	hb.-perid.	pxnt.	perid.	perid.	pxnt.	perid.	pxnt.	feld. pxnt.	px-rich gabbro	gabbro	gabbro	gabbro

Analyst: J. Mysson

*Repeated analysis: SiO_2 48.9%

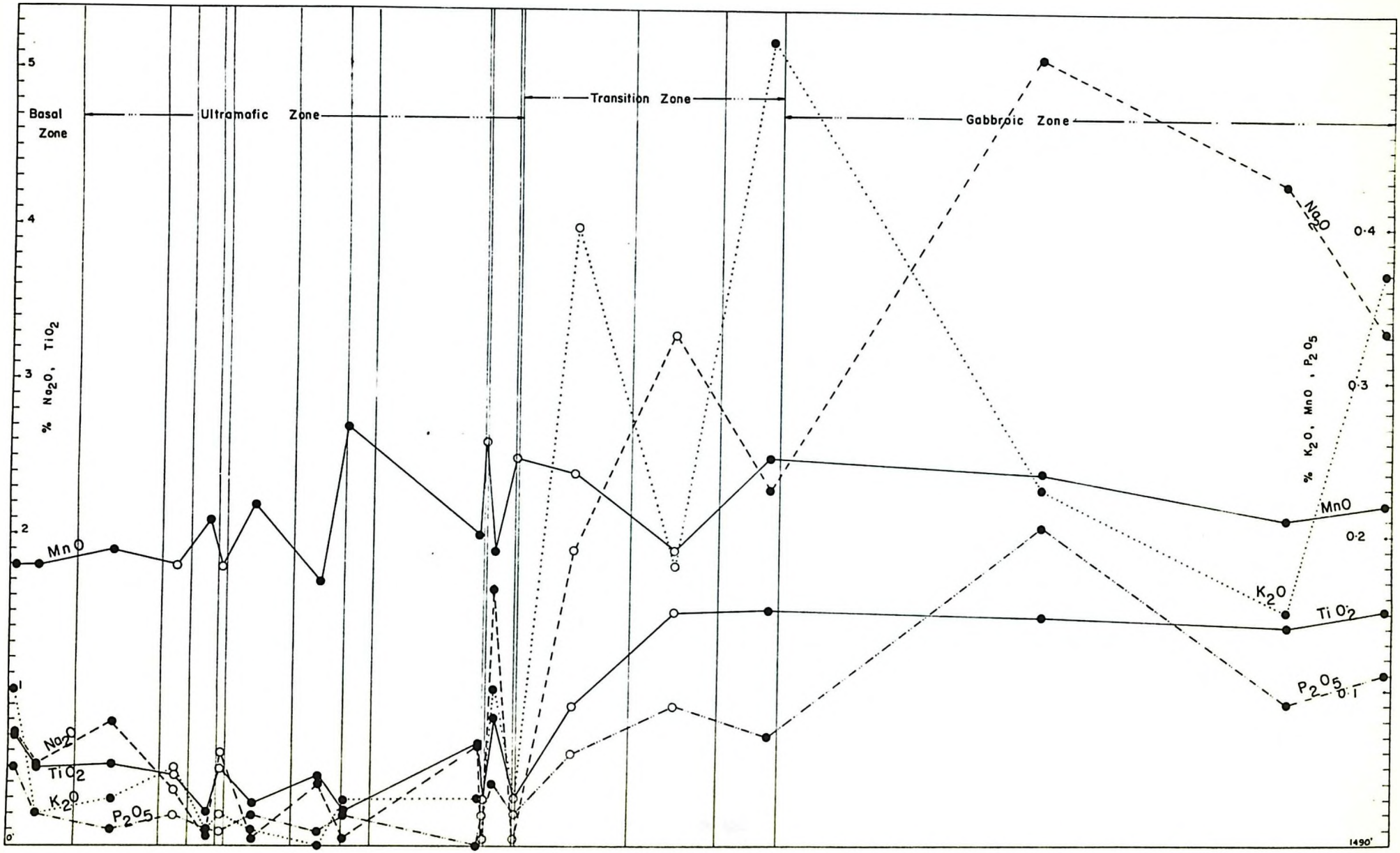

FIG. 23a

MAJOR OXIDE VARIATION DIAGRAM

● Chemical Analysis ○ Calculated Analysis

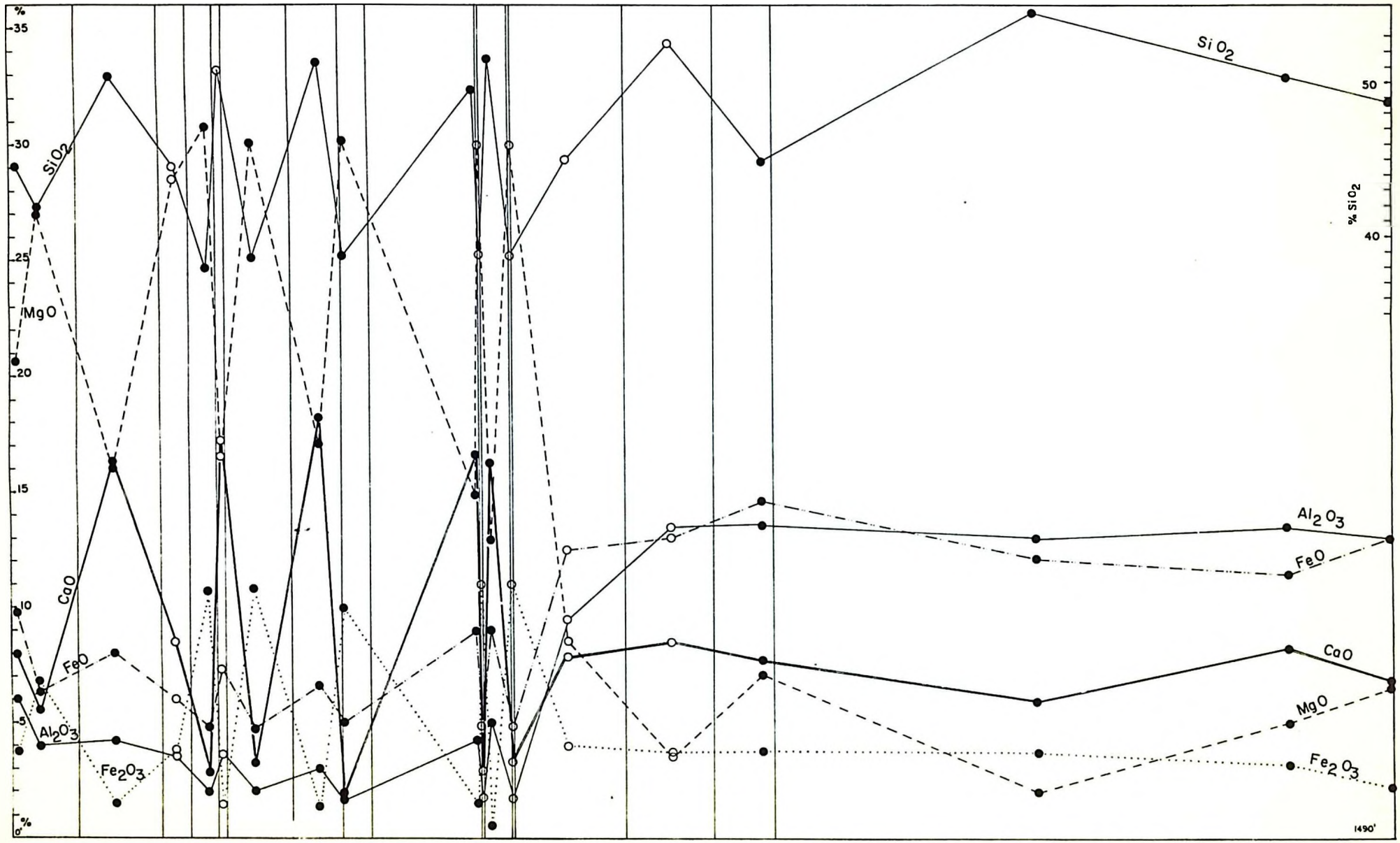

FIG. 23b

MAJOR OXIDE VARIATION DIAGRAM

● Chemical Analysis ○ Calculated Analysis

pyroxene are the major constituents and both are changing composition along their respective solid-solution series. Increases in amounts of one mineral, say, olivine over clinopyroxene, may be correlated with noticeable changes or trends in the element correlation plots. Peridotites may be assumed to consist of only clinopyroxene and olivine, the pyroxenites, of clinopyroxene with a gradual increase of plagioclase, and the gabbros, of plagioclase with an approximately equal amount of mafic silicates and fluctuating but significant quantities of opaques (oxides particularly).

From the Mn-Co plot of Plate 4A, it can be concluded that peridotites have a slight enrichment in cobalt but that the remainder show little discrimination. Pyroxenites and gabbros have approximately equal concentration of cobalt. The distribution of cobalt is completely dependent on the number of octahedral sites occupied by magnesium and iron (Turekian 1963), hence some concentration in the early phases must be expected. Manganese, which has diadochic substitution of Mn^{+2} for Fe^{+2} in a magma, shows greatest concentration in the magnetite-bearing samples.

The Ni-Cr plot of Plate 4B shows a general decrease in both elements from peridotite to pyroxenite to gabbro. A recent review of the Cr/Ni ratio of both the Stillwater rocks and basalts in general by Turekian (1963) reveals that the process of fractional crystallization of a basaltic magma does not significantly change the Cr/Ni ratio. A plot of chromium versus nickel for world-wide basalts (p. 840, Turekian 1963) gives an average Cr/Ni ratio of 1.29 and extremes of 0.46 and 4.25. Using the average chromium and nickel values for the Skaergaard rocks

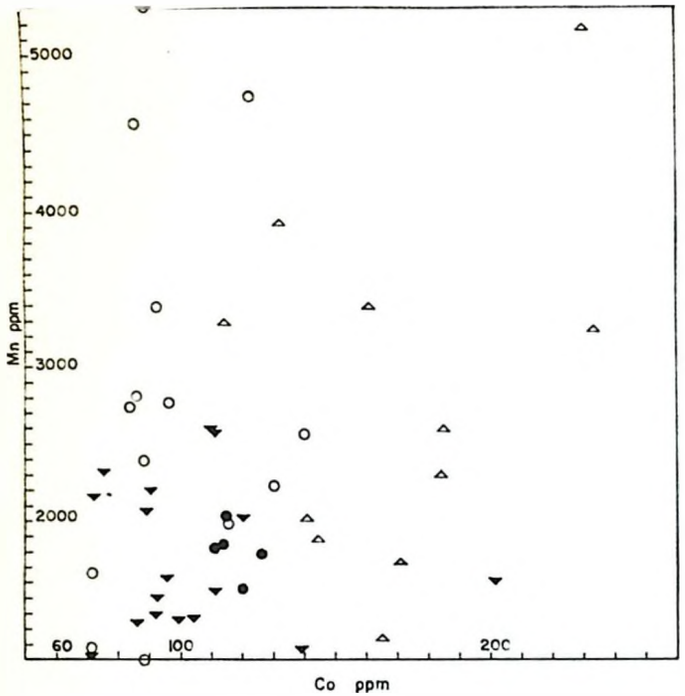

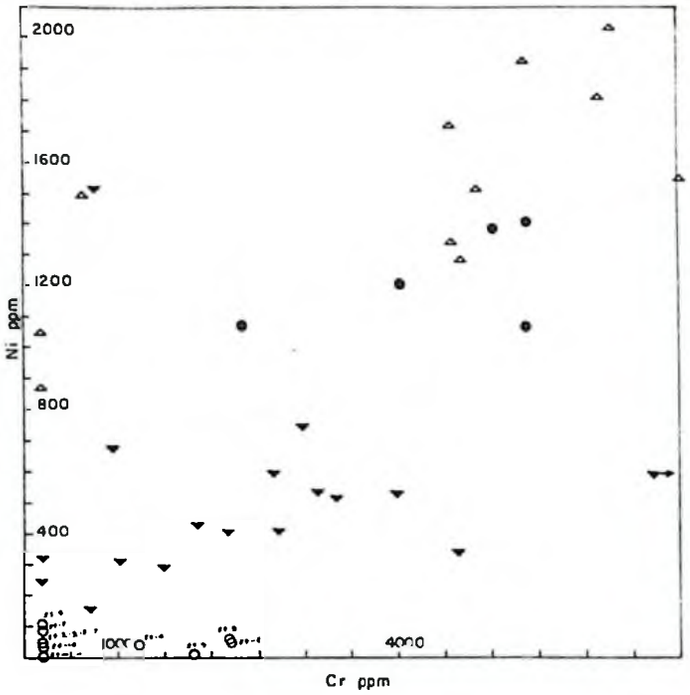

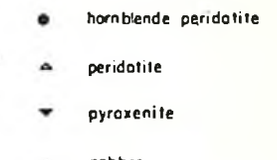

C

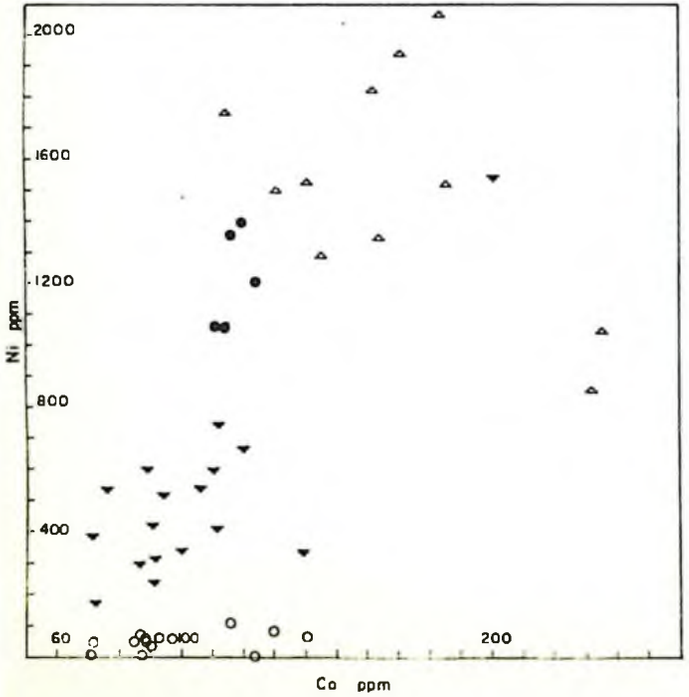

D

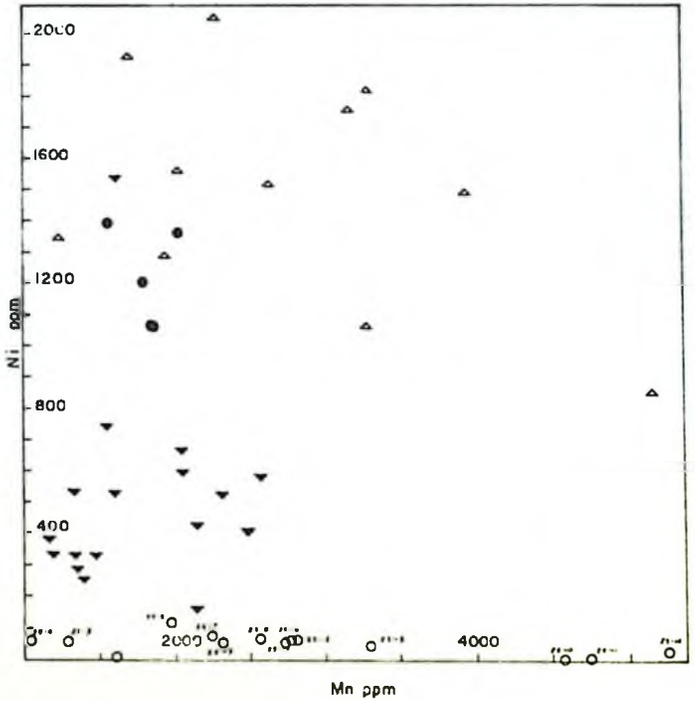

E

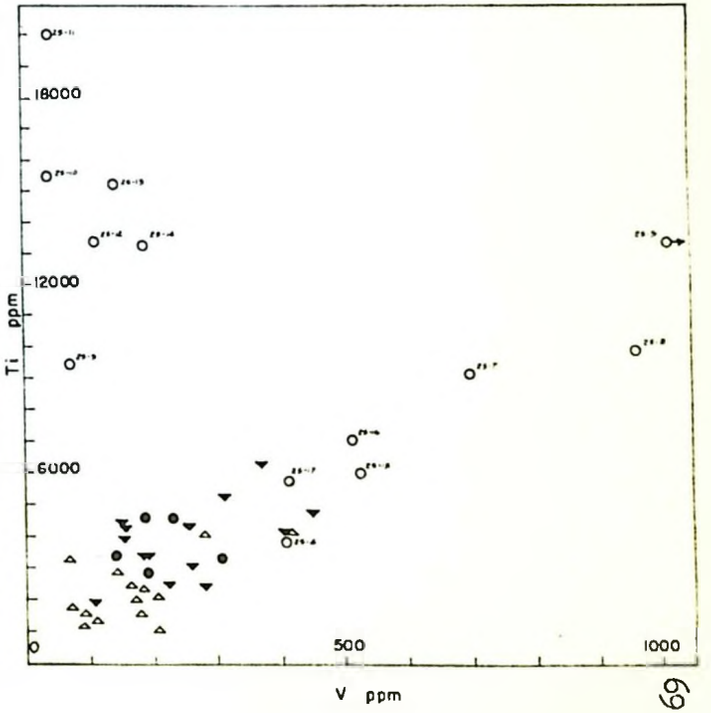

PLATE 4 - CORRELATION DIAGRAMS

(Wager and Mitchell 1951), Cr/Ni ratios from 1.2 to 1.9 are obtained. The Centre Hill ratio of 3.6 apparently indicates a considerable depletion of nickel in the primary magma.

Plate 4C, the Ni-Co correlation diagram, supports conclusions made above, namely that cobalt decreases slightly from peridotite to gabbro-pyroxenite and that nickel decreases markedly toward gabbro. Both the Skaergaard (Wager and Mithcell 1951) and the Stillwater (Turekian 1963) rocks exhibit the same trends.

A plot of nickel versus manganese (Plate 4D) shows good separation of the rock groups on the nickel scale and a wide range for all but pyroxenites on the manganese scale. The gabbro points, which are roughly aligned along a nickel value of approximately 50 ppm, are of interest since those with lowest manganese are the stratigraphically lowest (southern-most) gabbros, the middle manganese group are the stratigraphically highest (northern-most) gabbros, and the highest manganese group are the middle gabbros. The middle and late gabbros contain approximately 0.5% modal opaques of which most is magnetite. Apparently magnetite of the middle gabbros has a greater concentration of manganese than that of the other gabbros.

Peridotites and pyroxenites are low in both titanium and vanadium (Plate 4E). Ilmenite is the major titanium-bearing mineral in magmatic rocks while vanadium, in the form of V^{+3}, commonly proxies for Fe^{+3} in magnetite. Ilmenomagnetite and its alteration products are identified in the gabbro thin sections, thus the gabbro plots are of special interest. Two groups of gabbro points appear in the diagram; the first group has high titanium and low vanadium while the second shows an enrichment of both titanium and vanadium along a linear trend including both pyroxenites

and peridotites. When sample numbers are affixed to the points it is noted that the first group includes the stratigraphically lowest and highest gabbros. It is possible that optical study of polished sections of the gabbros would reveal more ilmenite in the middle layers than in other horizons.

CLASSIFICATION

Numerous attempts have been made to isolate exclusive parameters to distinguish between the two major types of gabbro-peridotite complexes, the stratiform and alpine types. No single criterion has yet proven completely satisfactory. Criteria are based on (i) orogenic environment, (ii) chemical composition of the parent magma, (iii) chemical and petrographic divisions within the intrusive body, and (iv) general form of the body.

STRATIFORM TYPE

The stratiform type, classically exemplified by the Skaergaard, Stillwater and Bushveld complexes, typically has a lopolithic to inverted cone shape, a chilled margin with a narrow but apparent metamorphic aureole, and an upward succession from ultrabasic to gabbroic and even granitic rocks. Compositionally, the border zone should be noritic. Dunite may be the lowest ultrabasic rock type, but typically pyroxene predominates over olivine and the rock type would be peridotite. A pyroxenite layer is common between lower peridotite and upper gabbro. Reversals of the normal peridotite-pyroxenite-gabbro sequence along any complete cross-section are usual. The interbanded zone typical of the beginning of some sequences is traceable along strike for great distances.

Stratiform complexes, as the name implies, are layered. The conspicuous banding which is apparent over much of each complex is

termed 'rhythmic' layering because of its rhythmic repetition. Variations in the relative percentages of more mafic and less mafic minerals are, of course, responsible for the layering. Cryptic layering, the gradual change in composition of the solid solution series of minerals, is an essential feature of stratiform complexes. Igneous lamination, the planar orientation of lath-like crystals may or may not be apparent.

Hess (1938) added a compositional criterion for the recognition of stratiform bodies; after a detailed study of the Mg/Fe ratio of the different rock sequences of both major genetic types, he states:" It can be concluded that low ratios, below 6, are almost certainly not members of the primary ultramafic (alpine type) magma series''.

The tectonic environment of stratiform plutons are commonly non-orogenic plateau areas.

ALPINE TYPE

A summary of alpine type characteristics becomes merely a list of negative statements directly opposed to the features of stratiform type intrusions. Lacking are a compositionally different border zone, any regular sequence of chemical or petrographic features and uninterrupted traceable petrographic horizons. Dunite rather than peridotite is the most common ultramafic rock type, and chromite, which tends to be concentrated along a few narrow horizons in a stratiform body, is more uniformly distributed in alpine bodies. Commonly, long and narrow sills in active orogenic belts are distinctive of alpine plutons.

CENTRE HILL CLASSIFICATION

The Centre Hill complex is, as stated earlier, merely a raised section of a long sill, the exact length of which is unknown. Numerous

highly folded and faulted sill segments occur in the immediate area and a comprehensive structural study has yet to be made.

Both lower and upper contacts show some chilling of the intrusion and baking of the country rocks, and, although these effects have not been studied in detail, metamorphism appears to be low grade (greenschist facies) and fades out rapidly in a nearly equivalent regional metamorphism. The basal zone of hornblende peridotite, while not noritic in composition, is less mafic than the preceding ultramafic layers. The top of the Gabbroic Zone is a hornblende gabbro which is only slightly more mafic than the preceding layers, and cannot be classed as a chilled margin.

Since a chilled margin should be direct evidence of the composition of the primary magma, a comparison of the basal hornblende peridotite composition and the calculated primary magma composition (see magma calculations in the following section) is shown in Table XV.

TABLE XV. Composition of Basal Layer Compared with Primary Liquid and Derived Composition of 'Chill Zone'.

	Calc. Primary Magma	Basal Peridotite 24-08	70% Magma + 30% Olivine Fo 77.5
SiO_2	50.96	47.27	47.32
TiO_2	1.10	.74	.77
Al_2O_3	9.72	6.40	6.80
Fe_2O_3	4.07	3.93	2.85
FeO	10.90	10.31	15.61
MnO	.22	.19	.15
MgO	11.04	21.83	18.12
CaO	8.92	8.39	6.24
Na_2O	2.79	.76	1.95
K_2O	.19	.10	.13
P_2O_5	.09	.05	.06

A recent experiment conducted at the GSC Ottawa Laboratories (Irvine, Personal Communication) helps to explain the occurrence of olivine in a marginal phase. After placing a layer of fragments of various sizes of a homogeneous material in a cylinder containing oil, the plunger-bottom of the cylinder was slowly pushed upward. The coarse fragments were found to migrate to a center axis position of the cylinder with the finest fragments toward the cylinder walls. The experiment was intended to simulate an intrusion of magma (liquid + crystals) into a chamber.

At Centre Hill the basal hornblende peridotite consists of very small and partially resorbed olivine crystals held within hornblende grains. The composition of the primary liquid should thus be represented by the hornblende peridotite composition minus a certain amount of olivine. A reasonably good approximation to the hornblende peridotite composition is obtained by adding 30 percent olivine $Fo_{77.5}$ (composition of samples 24-10 and 24-11) to 70 percent primary liquid (Table XV). Such differences as do exist may be results of migration of elements during metamorphism, or by early contamination by diffusion from the wall rocks.

As indicated in Figure 20, the mineral variation diagram, cryptic layering is present and rock type reversals, particularly in the Ultramafic Zone are common. The consistent trend in lithology, however, is from peridotite, rich in magnesium-olivine, to quartz-bearing gabbro.

In the Transition Zone a narrow but traceable zone of igneous lamination of feldspars at a reversal stage is one of the most striking petrographic features.

It is hardly necessary that every discovered mafic-ultramafic complex must fall in either one of the pure end-member groups, stratiform or alpine. However, it seems clear that the Centre Hill complex is very close to a pure differentiated or stratiform type.

Satterly, in his Munro Township report (1951), calls the Centre Hill body a differentiated sill, but Taylor (1955) postulated a more complex origin and classification close to alpine type. Grubb (1962) gave the mafic and ultramafic rocks of this belt an undoubtedly alpine classification.

Taylor's theory of origin and statements of classification were based, as were the author's, on both chemical and petrographic data. Unfortunately, however, Taylor's chemical data were calculated compositions using the Rosiwal analyses techniques. With no wet chemical analyses as guide and inadequate mineralogical work, sufficient errors were introduced such that no trace of cryptic layering was found.

Using Hess' criterion of Mg/Fe ratio, Taylor obtained 12.4 for a serpentinized dunite, 8.5 for a serpentinized peridotite, and 6.6 for a pyroxenite. The location of the specimens used for this test is not known, but it is assumed they must be in rocks related in origin to the Centre Hill complex. At Centre Hill Mg/Fe ratios from peridotites give a range of 2.44 to 3.38, certainly lower than the maximum limit of 6 suggested by Hess for stratiform type plutons.

DIFFERENTIATION

Once the assumption of a closed system of magma is made, some workable theory of differentiation must be presented. Clearly, this theory must explain both chemical and physical features observed.

The primary chemical feature is the cryptic layering of olivine, pyroxene and plagioclase, while the principal physical features are the general sequence from peridotite to pyroxenite to gabbro with frequent repetitions and sharp contacts of each band. Other points are significant, but these are the most striking.

MECHANISM OF DIFFERENTIATION

Gravity Sinking

The sequence peridotite-pyroxenite-gabbro at once suggests the possibility of the operation of gravity to separate the minerals. No problem arises from the separation of plagioclase crystals from pyroxene or olivine in a moderatly viscous fluid since the specific gravity of plagioclase ranges from 2.61 to 2.76, that for pyroxene from 2.8 to 3.7, and for olivine from 3.2 to 4.4 (Winchell and Winchell 1951). The overlap of specific gravities for olivine and pyroxene requires close examination.

As olivine and pyroxene crystallize from a magma, their compositions should gradually change from magnesium-rich toward iron-rich, assuming crystallization in a closed system. Since the specific gravity of each mineral varies directly as the molar percentage of iron silicate contained

in the mineral cell, the specific gravity is known approximately once the composition is determined, or vice versa.

Coates (1936) gives an excellent explanation of rhythmic banding effected simply by gravity. Both pyroxene and plagioclase, for example, will sink slowly to the floor of a chamber in which the magma is very slightly less dense than plagioclase. However, the rates of settling will differ somewhat, pyroxene settling faster than plagioclase. The sinking crystals must displace an equal amount of fluid as they settle, and the resultant slight upward current will tend to hold the less dense phase (plagioclase) off the chamber floor. As the layer of suspended plagioclase crystals thickens, the openings through which pyroxene grains slip gradually close, so that pyroxene grains cover the feldspar layer, which settles into place on the chamber floor as the vertical opposing currents lessen.

Current Action

Simple gravity sinking of crystals explains the common upward sequence from peridotite through pyroxenite to gabbro and even the small-scale layering contained therein. However, other physical phenomena are not so simply explained. Evidence of current action somewhere within each complex is usually found. Wager and Deer (1939) found abundant flow structure in the Skaergaard rocks, from trough banding to winnowed crystals and thickened layers of heavy mineral concentrations at the edges of the chamber. With respect to the orientation of platey crystals of plagioclase, they state:

> ... direct sinking would produce little or no parallelism of the crystals owing to the feebleness of the orienting forces. On the other hand if the magma were undergoing gentle flow there would be an orienting force easily sufficient to lay out the minerals with their flat expanses parallel to the surface of the accumulating pile of crystals, and this direction would also be parallel to the direction of flow of the magma.

The now classical theory outlined by Wager and Deer to explain the very evident effects of flow is widely accepted. Using the well-known fact that magmas tend to crystallize from the edges inward, they reason that the top of the chamber will be the most effective cooling area and thus the most efficient crystallization zone. The crystal plus fluid phase which forms near the top of the chamber must have a density higher than the underlying magma. (Hess suggests that the Stillwater magma had an original density of 2.65 g/cc at 1125°C.) For a time this upper zone will be partially supported, but as the crystal load grows the whole top layer will become unstable and sweep toward the side and bottom of the chamber. The downward movement of this mass must be opposed by an upward current near the center of the chamber. Such convection currents are well suited to the shape of the Skaergaard chamber since the ideal containing cell for an operating convection current is one where the horizontal dimension only slightly exceeds the vertical (Hess 1960).

Variation of Magma Composition

Wager and Deer (Skaergaard complex), Hess (Stillwater complex) and Hall (Bushveld complex) assume that the initial magma for these three plutons was intruded into its present site in one major surge, and that thereafter each system may be assumed closed to all components except, perhaps, H_2O, CO_2 and O_2, during the periods of differentiation.

Large-scale oscillations in rock types can be explained by current movements in the case of a large chamber such as the Skaergaard. However, a sharp and major reversal from less mafic to more mafic composition for extensive and remarkably uniform layers is hard to explain by current action in thin tabular bodies. It seems inevitable that changes in the

composition of the crystallising magma must be responsible for the changes in rock types.

Two methods of effecting such changes have been suggested. Yoder (1954) has shown experimentally that the diopside-anorthite eutectic is readily influenced by small alternations of the pH_2O of the system. Volatiles periodically escaping from the system via fractures in the chamber walls could bring about mafic reversals in the crystallization zone. A more effective method is to simply introduce new material to the magma. Assimilation of wall rock is ineffective for such mafic reversals but addition of new magma, i.e. multiple injection from a basaltic reservoir, is a possibility heavily supported by Cooper (1936) and Lombard (1935). Repeated surges of basaltic magma into the main chamber are thought by Irvine (Personal Communication) to be responsible for the major oscillations of rock sequences in the Muskox complex (Northwest Territories).

DIFFERENTIATION OF CENTRE HILL MAGMA

Mechanism of Differentiation

Taylor contested the idea of gravity banding for the Haileyburian ultramafic rocks because of the close similarity of density of diopside (3.33) and forsterite (3.32). Petrographic study of the Centre Hill rocks show that the olivine is not pure forsterite and the pyroxene is augite, not diopside.

Approximate specific gravities for both minerals are listed in Table XVI opposite each composition determination.

Quite obviously, the specific gravities of any contemporaneous olivine and pyroxene are sufficiently different that gravity separation of the minerals in a magma chamber is possible.

TABLE XVI. Specific Gravities of Olivines and Pyroxenes.
Olivine Ref: Deer, Howie, Zussman (1962) Vol. 1.
Pyroxene Ref: Winchell and Winchell (1951) Assuming Constant Wo.

Sample No.	Olivine Composition	S.G.	Clinopyroxene Composition		S.G.
24-10	Fo 77.5	3.45			
24-11	Fo 77.5	3.46			
24-13			En 44	Fs 06	3.3
24-15			En 42	Fs 06	3.3
24-16	Fo 74.5	3.47			
24-21			En 42	Fs 09	3.3
24-25	Fo 72.5	3.51			
24-26			En 41	Fs 10	3.31
24-30	Fo 75	3.47			
24-31	Fo 69.5	3.53			
24-32			En 40	Fs 11	3.31
24-34	Fo 64.3	3.60			
24-36			En 45	Fs 06	
24-37	Fo 64	3.61			
25-01			En 40	Fs 13	3.35
25-08			En 40	Fs 22	3.38
25-10			En 37	Fs 26	3.40
25-16			En 38	Fs 26	3.40

With regard to the importance of current action, the tabular shape of the Centre Hill sill makes the operation of large convection cells difficult. However, some current action must undoubtably have aided in the formation of the rocks, as evidenced by the planar orientation of feldspar crystals in the Transition Zone. In the gabbros above the Transition Zone tabular crystals have an apparently random orientation, thus current action during crystallization of the Gabbroic Zone may be assumed negligible.

The extensive repetition of the peridotite-pyroxenite cycle throughout the Ultramafic Zone coupled with the fact that large-scale convection cells could not be operative lead to the conclusion that the differentiation was chemically controlled. Direct evidence for the addition of new material to the crystallization zone is absent. However, the reversals in composition of olivine from decreasing forsterite to an abrupt increase in sample 24-30, and of clinopyroxene from increasing ferrosilite to a similarly abrupt decrease in sample 24-36 are good points of indirect evidence.

The composition of the added material need not be different from that of the original primary injection. If the new injections are not large or frequent the dilution effect of the main magma will still allow cryptic layering in the crystallized products.

The trend of differentiation of the Centre Hill complex can be attributed to two main phenomena; firstly, the continuous action of gravity on the crystallizing components, and secondly, the periodic resurgence of basaltic material into the chamber of crystallization. The noted occurrences of rhythmic layering - a gravity effect - and cryptic

layering - an effect of crystal fractionation - are thus readily explainable, with the need to introduce mild current action only to explain the igneous lamination of the Transition Zone.

The lack of anorthositic, or more acidic, dikes indicates that there has been little expulsion of late residual material.

Crystallization Trend

Assuming crystal formation at the top of the chamber and solidification from the bottom upward, it is difficult to interpret, in particular, the trend of quartz in the mineral variation diagram of Figure 20. The suggestion of partial solidification from the top of the chamber downward is immediately obvious and must be tested.

It is significant that the Ni-Mn and Ti-V correlation diagrams of Plate 4 show grouping of both stratigraphically highest and lowest gabbros but divergence of the middle gabbros. Further evidence is available from the triangular FeO-MgO-(K_2O + Na_2O) plot showing the positions of whole-rock analyses (Figure 24). Sample 25-12, a middle gabbro, is furthest along a tholeiitic trend, the three other gabbro points showing less extreme differentiation.

The middle of the Gabbroic Zone can, apparently, be taken as the last crystallized section of the Centre Hill complex. Solidification from the top downward probably did not commence until the chamber narrowed to such an extent that the circulating currents (evidenced by igneous lamination in the Transition Zone) had ceased.

COMPOSITION OF SUCCESSIVE MAGMAS

For ease of calculation, and from lack of knowledge concerning the dimensions of the original sill, measured thickness (i.e. true

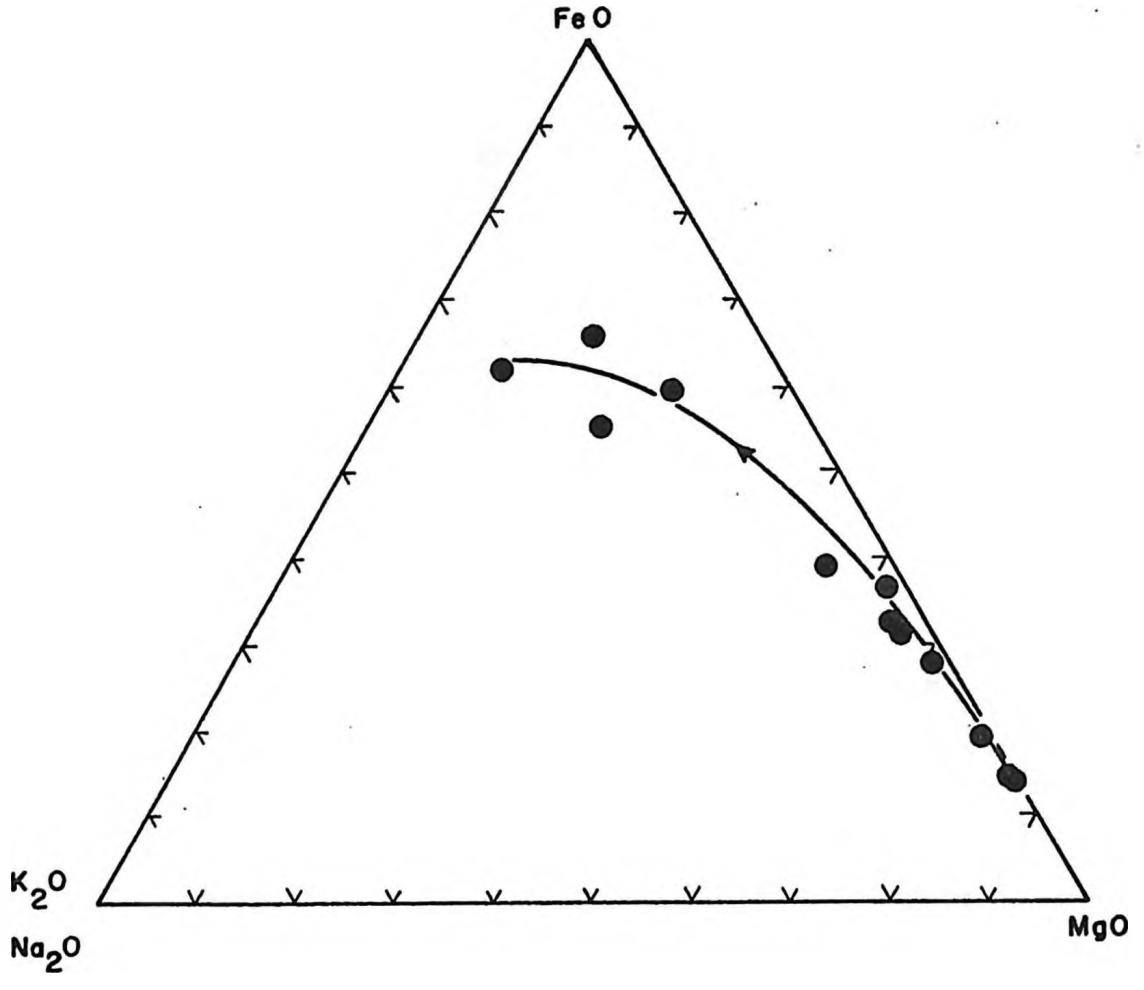

Figure 24. Trend of Centre Hill rocks on FeO-MgO-total alkali diagram.

thickness) of layers is assumed directly proportional to volume. With the further assumption of no squeezing out of any residuum, the composition of the last 'liquid' or magma must be completely equivalent to the composition of the last-formed rock. The second-last magma will have a composition equivalent to the composition of the last formed rock multiplied by its thickness plus the composition of the second-last formed rock multiplied by its thickness, all recalculated to 100 percent. Successive liquids can be calculated similarly until the whole intrusion section has been accounted for.

Successive magma compositions are summarized in Table XVII with respective norms, as weight percents, listed in Table XVIII. The various steps of successive magma calculations are detailed in the Appendix.

Sample 25-12 is the most acidic member of the gabbro group and appears to represent the last crystallized phase. The remaining gabbros form a fairly homogeneous unit. Hence, the second-last magma accounts for the whole Gabbroic Zone. The two 3-foot peridotite layers, Units 10 and 12, have been combined with Unit 8 for ease of calculation. For those units where chemical analyses were not available, compositions were calculated on the basis of mineralogical and spectrographic data.

Figure 25 shows the liquid trend of Centre Hill magmas on a MgO-FeO-(Na_2O + K_2O) diagram.

VOLATILE CONTENT OF MAGMA

Autometasomatism of differentiating basaltic magmas is a popular theory of many petrologists. The amount of water required in such a process to serpentinize completely or nearly completely large amounts

TABLE XVII. Composition of Successive Magmas.

	Final Magma	14th Magma	13th Magma	12th Magma	11th Magma	10th Magma	9th Magma	8th Magma
SiO_2	55.34	53.79	52.92	52.87	52.46	52.46	52.29	52.01
TiO_2	1.49	1.49	1.50	1.50	1.44	1.42	1.34	1.31
Al_2O_3	13.20	13.40	13.49	13.49	13.11	12.87	11.94	11.63
Fe_2O_3	3.76	3.44	3.50	3.52	3.63	3.54	3.33	3.63
FeO	12.29	12.32	12.66	12.70	12.84	12.73	12.35	12.13
MnO	.24	.23	.23	.23	.23	.23	.23	.23
MgO	2.03	3.43	3.91	3.86	4.55	4.81	5.95	6.83
CaO	5.99	6.72	6.87	7.06	7.25	7.54	8.57	8.37
Na_2O	5.22	4.78	4.49	4.35	4.07	3.99	3.63	3.52
K_2O	.23	.23	.27	.26	.28	.28	.25	.24
P_2O_5	.21	.17	.16	.15	.14	.13	.12	.12

	7th Magma	6th Magma	5th Magma	4th Magma	3rd Magma	2nd Magma	Primary Magma
SiO_2	52.01	51.54	51.51	51.30	51.19	51.21	50.96
TiO_2	1.27	1.21	1.21	1.18	1.17	1.13	1.10
Al_2O_3	11.23	10.74	10.67	10.48	10.33	9.95	9.72
Fe_2O_3	3.51	3.98	3.96	4.14	4.13	3.97	4.07
FeO	11.88	11.52	11.48	11.34	11.23	11.04	10.90
MnO	.23	.23	.23	.23	.23	.23	.22
MgO	7.31	8.77	8.83	9.42	9.87	10.27	11.04
CaO	8.84	8.56	8.63	8.50	8.51	9.02	8.92
Na_2O	3.37	3.19	3.17	3.10	3.03	2.90	2.79
K_2O	.23	.22	.22	.21	.21	.20	.19
P_2O_5	.11	.11	.11	.10	.10	.10	.09

TABLE XVIII. Normative Mineralogy of Successive Magmas (Weight Percent)

	Primary Magma	2nd Magma	3rd Magma	4th Magma	5th Magma	6th Magma	7th Magma	8th Magma
Quartz	-	-	-	-	-	-	0.26	0.36
Orthoclase	1.12	1.18	1.24	1.24	1.30	1.30	1.36	1.42
Albite	23.60	24.53	25.64	26.23	26.81	26.97	28.51	29.78
Anorthite	13.44	13.54	13.97	14.06	14.23	14.33	14.84	15.23
Diopside	16.55	16.25	14.45	14.10	13.83	13.60	12.80	11.12
Hypersthene	8.00	8.62	8.05	8.33	8.94	8.85	10.57	10.01
Enstatite	15.77	15.15	15.42	15.13	14.50	14.54	12.27	11.85
Ferrosilite	8.74	9.22	9.85	10.25	10.71	10.85	11.63	12.23
Forsterite	2.84	2.02	1.72	1.25	0.74	0.69	-	-
Fayalite	1.74	1.35	1.21	0.93	0.60	0.57	-	-
Magnetite	5.90	5.75	5.99	6.00	5.74	5.77	5.09	5.23
Ilmenite	2.09	2.15	2.22	2.24	2.30	2.30	2.41	2.49
Apatite	-	0.23	0.23	0.23	0.26	0.25	0.26	0.28

	9th Magma	10th Magma	11th Magma	12th Magma	13th Magma	14th Magma	Final Magma
Quartz	0.75	1.14	1.28	1.54	1.05	1.84	4.43
Orthoclase	1.48	1.66	1.65	1.54	1.60	1.36	1.38
Albite	30.72	33.76	34.43	36.81	37.99	40.44	44.15
Anorthite	15.55	16.38	16.68	16.52	15.86	14.43	11.90
Diopside	10.53	7.21	6.35	5.56	5.50	5.37	3.53
Hypersthene	11.28	9.73	9.11	9.26	9.02	9.72	10.60
Enstatite	9.89	8.63	8.39	7.04	7.19	6.05	3.42
Ferrosilite	12.15	13.36	13.79	13.44	13.51	12.58	11.81
Forsterite	-	-	-	-	-	-	-
Fayalite	-	-	-	-	-	-	-
Magnetite	4.83	5.13	5.26	5.10	5.07	4.99	5.45
Ilmenite	2.55	2.70	2.73	2.85	2.85	2.83	2.83
Apatite	0.28	0.30	0.32	0.35	0.37	0.39	0.49

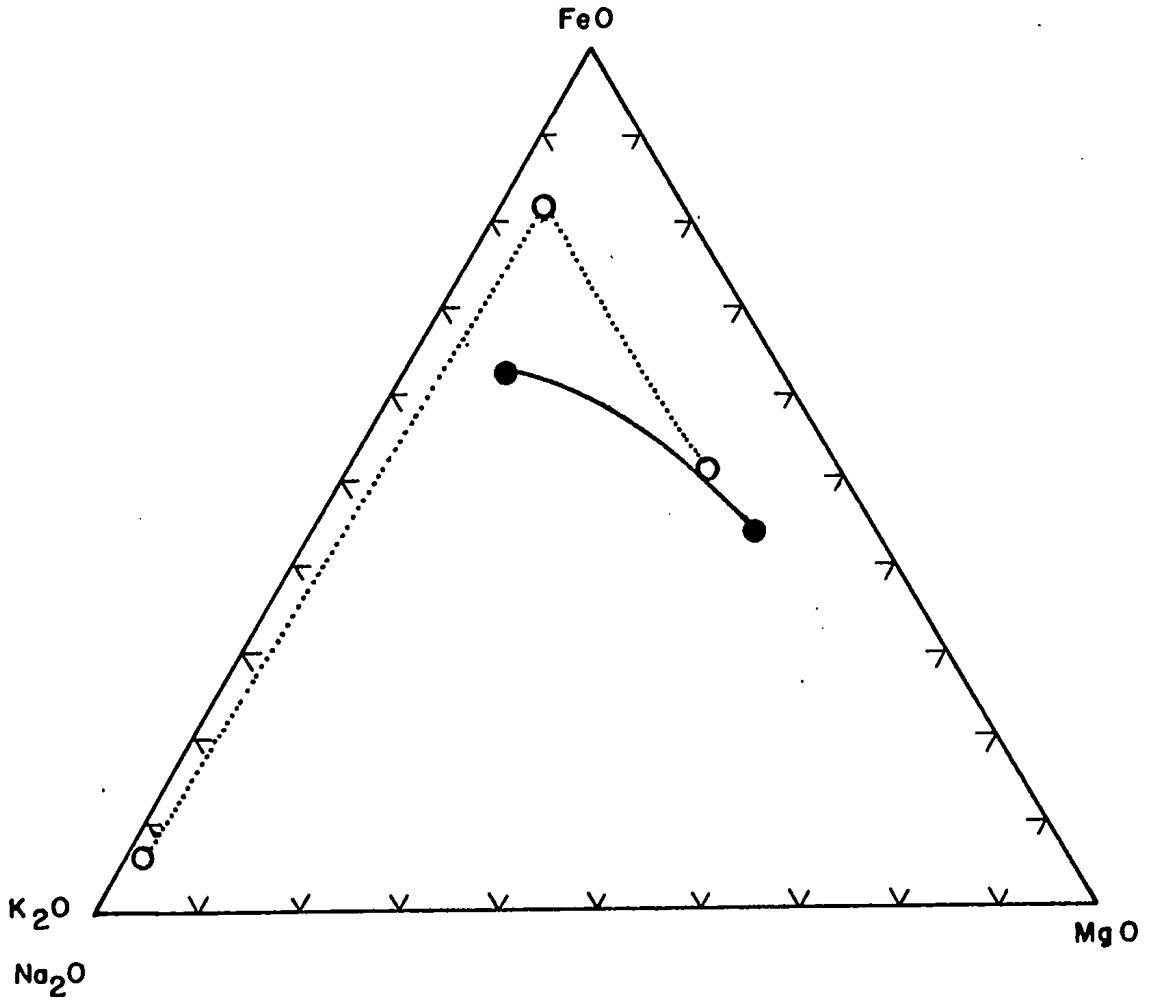

Figure 25. Successive magma trend plotted on MgO-FeO-total alkali diagram. Solid line - Centre Hill and first and last magma points shown. Dotted line - Skaergaard and first, fourth and seventh shown.

of olivine is exceedingly great. To propose that such volumes of water could be indigenous is, in most cases, out of the question.

It must be remembered that the best indicators of a magma's water content are the primary minerals which it precipitates. A water-rich basaltic magma would begin crystallizing hornblende early, interstitial hornblende appearing in peridotites and pyroxenite, and primary hornblende crystals in gabbro. Most excess water would be used up in this manner, leaving little at any stage for autometasomatism. If the same magma were, for some theoretical reason, to crystallize olivine, pyroxene and plagioclase and not hornblende, it would undergo second boiling and lose the water before it cooled to temperatures where autometasomatism would occur.

At Centre Hill the remnant red-brown hornblende of the Basal Zone and the euhedral to subhedral light green hornblende of the Gabbroic Zone are considered to be primary magmatic phases. No interstitial hornblende occurs in the pyroxenites with the exception of a slight residual of red-brown hornblende in the first unit above the Basal Zone. The basal hornblende indicates a slightly water-rich magma, but apparently the excess water was quickly used up since normal pyroxene-olivine-plagioclase mineralogy is assumed above the Basal Zone. The hornblende gabbros do not form continuous layers in the Gabbroic Zone, but are rather elongate lenses at various horizons. Possibly these occurrences represent pockets in which the water content was high.

DISCUSSION OF DIFFERENTIATION TREND

The primary magma compositions for Centre Hill, Stillwater, Bushveld and Skaergaard are shown in Table IXX. The notable differences

TABLE LIX. Composition of Primary Magma of Stratiform Complexes. A,B: Green and Poldervaart, 1955; C: Wager and Deer, 1939.

	A Stillwater	B Bushveld	C Skaergaard	Centre Hill
SiO_2	50.9	52.0	47.92	50.96
TiO_2	0.5	0.8	1.35	1.10
Al_2O_3	17.7	15.5	18.86	9.72
Fe_2O_3	0.3	1.9	1.18	4.07
FeO	10.0	8.0	8.66	10.90
MnO	0.2	0.2	0.10	0.22
MgO	7.7	8.5	7.82	11.04
CaO	10.5	10.6	10.46	8.92
Na_2O	1.9	1.8	2.44	2.79
K_2O	0.2	0.6	0.18	0.19
P_2O_5	0.1	0.1	0.07	0.09

(high MgO and low Al_2O_3) in the Centre Hill magma are not likely to be metasomatic effects from serpentinizing fluids. According to Yoder and Tilley (1962), a rock of such composition and normative mineralogy as noted in Table XVIII, would be classified as an olivine tholeiite.

The equilibrium diagram of the system FeO-MgO-SiO_2 (Figure 26) can be used to roughly outline the course of crystallization. From a primary magma point 'x' a fractional crystallization trend would intersect the pyroxene field at 'y'. Instead of following the curve 'KL', as in non-fractional processes, the liquid crosses the pyroxene field in a curved path (with continual separation of pyroxene of changing composition) to the pyroxene-silica boundary. Moderate fractional crystallization, as at Centre Hill, will commonly result in complete solidification when the liquid reaches a point between 'C' and 'L', but for strong fractionation, as for the Skaergaard liquid, the curve is followed to the reappearance of iron-rich olivine. The high temperature pyroxene to form under such magmatic conditions will be clinopyroxene. Exsolution

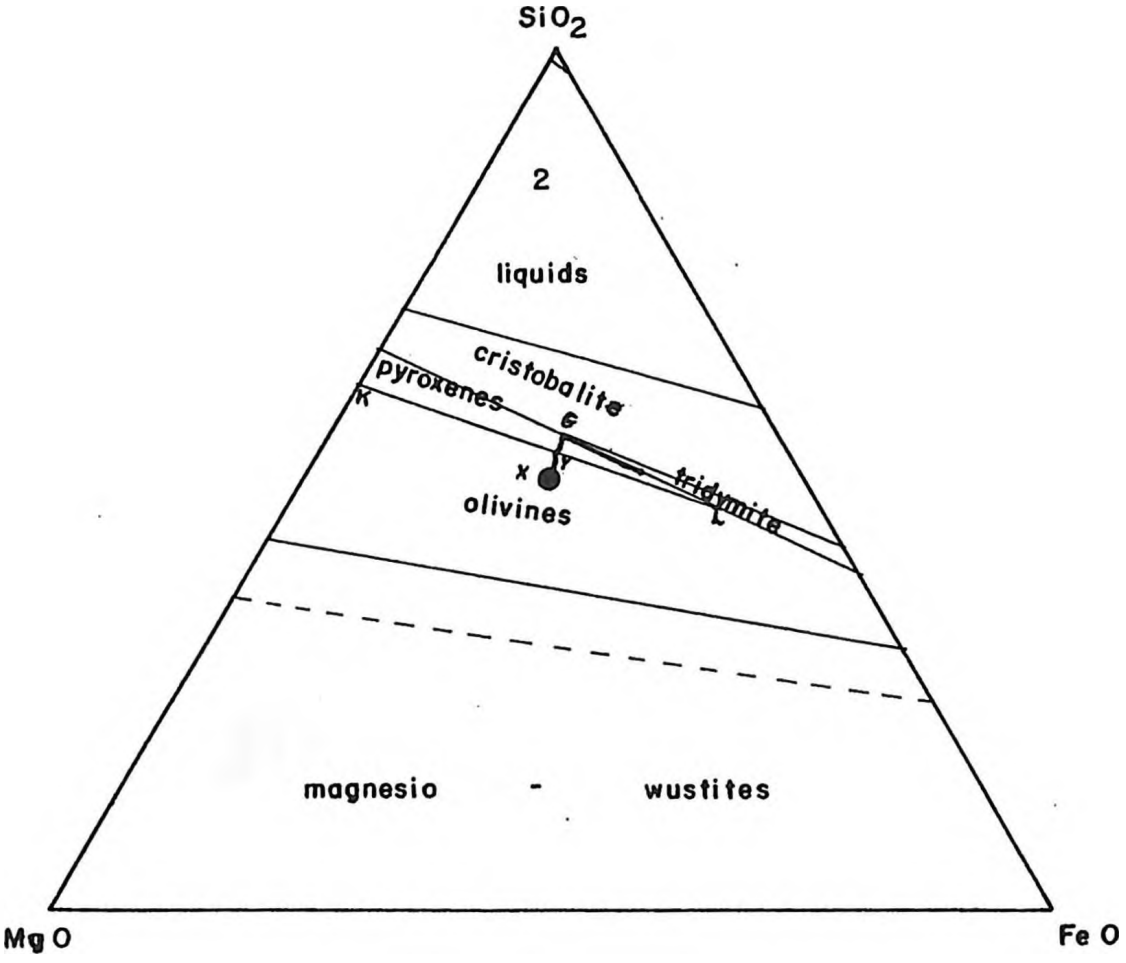

Figure 26. Moderately fractionated crystallization course similar to Centre Hill magma.

or complete conversion to an orthorhombic form at lower temperatures is common in stratiform deposits, but such did not happen at Centre Hill.

It is possible for clinopyroxene to be the reaction product of olivine by taking the 'normal' orthopyroxene reaction product into solid solution (Schairer and Yoder 1961-62), but excessively large 2V angles should indicate the amount of orthopyroxene in solid solution. The Centre Hill clinopyroxenes do not show unusually large 2V's.

A comparison of the differentiation trend under normal fractional crystallization and the projected approximate trend of the Centre Hill magma is shown in Figure 27. The pressure limitation of the triangular diagram is one atmosphere, and the compositional limitation is the lack of iron-silicates.

Changing composition of the magma due to resurging basaltic material caused oscillations across the olivine-pyroxene boundary, resulting in such phenomena as the two 3-foot-wide peridotite bands, Units 10 and 12. At a later stage of differentiation additional resurgence caused the oscillations mirrored by the interbanded gabbro of the Transition Zone.

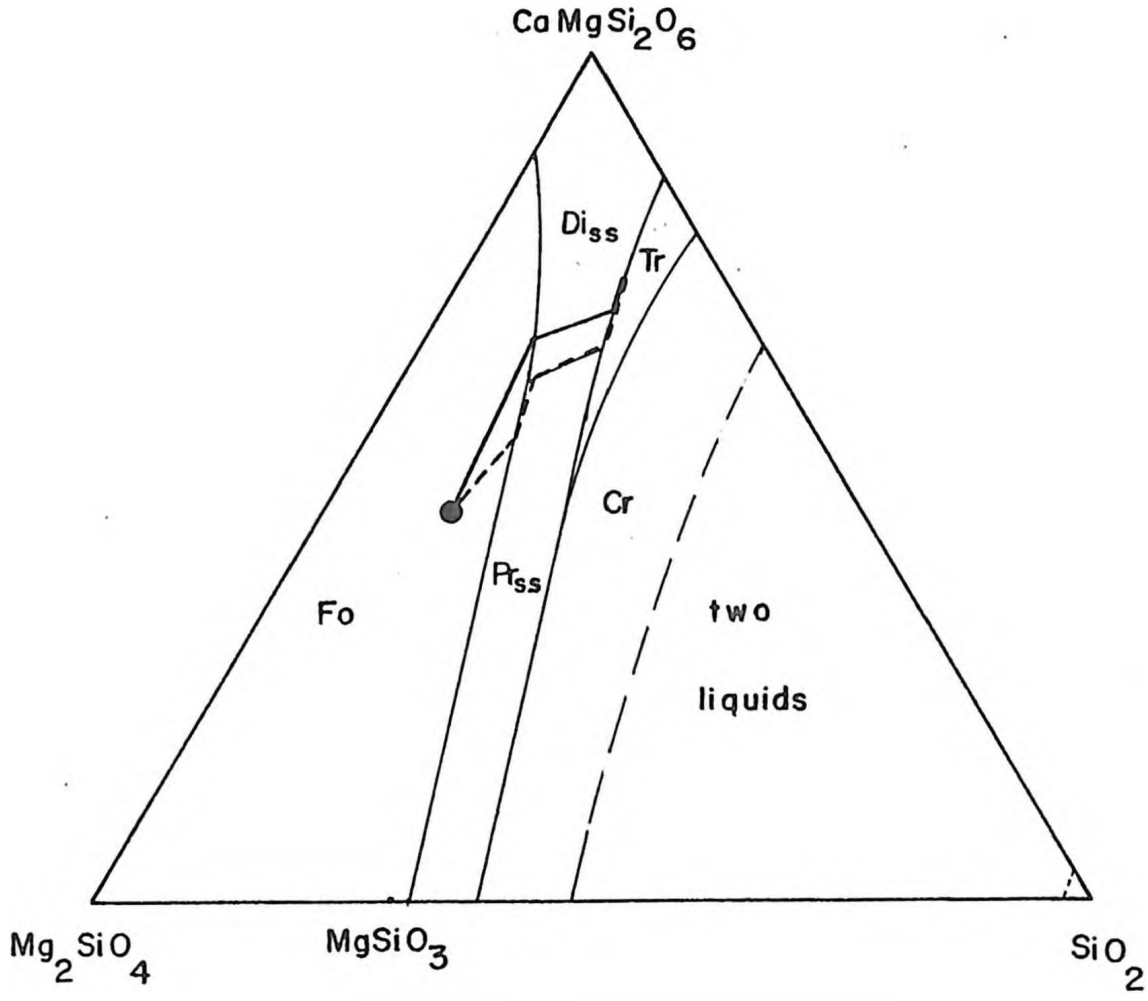

Figure 27. Liquidus diagram of system Di-Fo-SiO_2 (after Schairer and Yoder 1961-62). Dashed line - normal fractional crystallization trend. Solid line - approximate Centre Hill trend.

ORIGIN OF BASALT MAGMA

Prompted by laboratory observations on eclogites, Yoder and Tilley (1962) suggest that the two main types of basalt magma are formed from the differentiation of eclogites in the mantle. Segregation of the garnet phase will produce a tholeiite-type liquid while segregation of omphacite components would yield a liquid, at high pressure (i.e. from greater depth), which would produce an alkali-type magma at the surface.

Assuming that the upper mantle has a top layer of peridotite, as evidenced by inclusions of peridotite within basalt flows, Kushiro and Kuno (1963) propose that all basalt magmas can be formed by partial melting of the upper mantle. With only 2 to 9 percent partial melting basalt compositions can be obtained and the residual retains the composition of peridotite. At shallow depth within the mantle a local supply of heat may cause the incongruent melting of orthopyroxene, resulting in the development of tholeiitic basalt magma. The obvious difficulty in such a process is the derivation of sufficient heat to cause remelting and fusion. Mechanisms of severe crustal down-warping so as to produce low pressure zones and the development of mantle convection cells have been proposed with some success.

Whatever the mechanism, it must be concluded that only partial melting of a sub-crustal rock layer can yield magmas of basalt composition.

CONCLUSIONS

Field examination of the Centre Hill complex suggests a theory of origin by in situ differentiation of a basaltic magma. Petrologic study confirms this idea, thus tentatively establishing a classification for at least one sill of the Abitibi Peridotite Belt.

The history of the complex may be summarized as follows:

a. Major intrusion of a basaltic magma, containing slightly more water than ordinary, along a rhyolite-basalt contact. The magma, even during the period of intrusion, was crystallizing olivine, as indicated by its content in the narrow basal or 'chill' layer. Excess water was quickly used by the crystallization of hornblende rather than pyroxene in the Basal Zone.

b. Normal fractional crystallization of the magma was periodically interrupted by minor injections of fresh basaltic material. Each new injection is recorded in the accumulated rocks by a reversal to more mafic from less mafic mineralogy.

c. Crystallization took place mainly at the roof of the sill and gravity acted to produce rhythmic layering in the solidifying products on the chamber floor. Solidification from the top downward did not take place until the last stages of differentiation.

d. Serpentinization and tremolitization of the intrusive rocks took place well after the rocks had solidified. Serpentinization, in particular, took place along fractures, decreasing in intensity into the sill. The serpentinizing fluids may have come from a nearby Algoman granodiorite plug.

A major conclusion is that a successful case for stratiform classification has been made on the basis of only one cross-section of the sill.

SELECTED BIBLIOGRAPHY

Bowen, N. L., 1914: The Ternary System Diopside-Forsterite-Silica; Am. J. Sci., 4th ser., vol. 38, 207-64.

_____ and Schairer, J. F., 1935: The System MgO-FeO-SiO_2; Am. J. Sci., 5th ser., vol. 29, 151-217.

_____ and Tuttle, O. F., 1949: The System MgO-SiO_2-H_2O; Bull. Geol. Soc. Amer., vol. 60, 439-60.

Brown, G. M. and Vincent, E. A., 1963: Pyroxenes from the Late Stages of Fractionation of the Skaergaard Intrusion, East Greenland; J. Petr., vol. 4, 175-97.

Coates, R. R., 1936: Primary Banding in Basic Plutonic Rocks; J. Geol., vol. 44, 407-419.

Deer, W. A., Howie, R. A. and Zussman, J., 1962: Rock Forming Minerals; vol. 1, London, Longmans.

Dixon, W. J. and Massey, F. J., Jr., 1957: Introduction to Statistical Analysis; McGraw Hill.

Emmons, R. C., 1943: The Universal Stage; Geol. Soc. Am. Mem. 8.

Fenner, C. N., 1929: The Crystallization of Basalts; Am. J. Sci., vol. 18, 225-253.

Grubb, P. L. C., 1962: Serpentinization and Chrysotile Formation in the Matheson Ultrabasic Belt, Northern Ontario; Econ. Geol., vol. 57, 1228-1246.

Hall, A. L., 1932: The Bushveld Igneous Complex of the Central Transvaal; South Africa Geol. Survey Mem. 28.

Hess, H. H., 1933: The Problems of Serpentinization; Econ. Geol., vol. 28, 634-657.

_____ 1938: A Primary Peridotite Magma; Am. J. Sci., 5th ser., vol. 35, 321-44.

_____ 1941: Pyroxenes of Common Mafic Magmas, pt. 2; Am. Min., vol. 26, 573-94.

Hess, H. H., 1949: Chemical Composition and Optical Properties of Common Clinopyroxene, part 1; Am. Min., vol. 34, 621-666.

_____ 1955: Serpentines, Orogeny and Epeirogeny; Geol. Soc. Am., Special paper 62, 391-408.

_____ 1960: Stillwater Igneous Complex, Montana: Geol. Soc. Am. Mem., vol. 80.

Jackson, E. D., 1961: Primary Textures and Mineral Associations in the Ultramafic Zone of the Stillwater Complex, Montana; Geol. Sur. Prof. Paper 358.

Kerr, P. F., 1959: Optical Mineralogy; McGraw-Hill.

Kushiro, I. and Kuno, H., 1963: Origin of Primary Basalt Magmas and Classification of Basaltic Rocks; J. Petr., vol. 4, 75-89.

Lombaard, B. V., 1935: On the Differentiation and Relationships of the Rocks of the Bushveld Complex; Geol. Soc. South Africa Trans., vol. 37, 5-52.

Moorhouse, W. W., 1959: The Study of Rocks in Thin Section; Harper and Bros.

Poldervaart, A. and Taubeneck, W. H., 1960: Layered Intrusions; Int. Geol. Cong., Part XIII, 239-246.

Satterly, J., 1951: Geology of Munro Township; Sixth Ann. Rep. Ontario Dept. of Mines, vol. LX, part VIII.

Schairer, J. F. and Yoder, H. S., Jr., 1961: The System Diopside-Enstatite-Silica; Carnegie Inst. Wash. Yearbook 1961, 75-82.

Smith, C. H., 1958: Bay of Islands Igneous Complex, Western Newfoundland; Geol. Soc. Can. Mem. 290.

Taylor, F. C., 1955: The Petrology of the Serpentine Belt in the Matheson District, Ontario; Ph.D. Thesis, McGill University.

Thayer, T. P., 1960: Some Critical Differences Between Alpine-Type and Stratiform Peridotite-Gabbro Complexes; Int. Geol. Cong., Part XIII, 247-259.

Turekian, K. K., 1963: The Chromium and Nickel Distribution in Basaltic Rocks and Eclogites; Geochim. et Cosmochim. Acta, vol. 27, 835-846.

Turner, F. J. and Verhoogen, J., 1960: Igneous and Metamorphic Petrology; McGraw-Hill.

Vincent, E. A. and Phillips, R., 1954: Iron-Titanium Oxide Minerals in Layered Gabbros of the Skaergaard Intrusion, East Greenland; Geochim. et Cosmochim. Acta, vol. 6, 1-26.

Wager, L. R. and Deer, W. A., 1939: The Petrology of the Skaergaard Intrusion, Kangerdlugssvaq, East Greenland; Meddelelser om Grønland; vol. 105, No. 4.

_____ and Mitchell, R. L., 1951: The Distribution of Trace Elements During Strong Fractionation of Basic Magma - A Further Study of the Skaergaard Intrusion, East Greenland; Geochim. et Cosmochim. Acta; Vol. 1, 129-208.

_____ Vincent, E. A. and Smales, A. A., 1957: Sulphides in the Skaergaard Intrusion, East Greenland; Econ. Geol., vol. 52, 855-903.

_____ 1960: The Major Element Variation of the Layered Series of the Skaergaard Intrusion and a Reestimation of the Average Composition of the Hidden Layered Series and of the Successive Residual Magmas; J. Petr., vol. 1, 364-98.

Wahlstrom, E. H., 1955: Petrographic Mineralogy; John Wiley and Sons.

Watkinson, D. H., 1963: Petrochemistry of the Mafic-Rich Rocks, Lac des Mille Lacs Area, Northwestern Ontario; M.Sc. Thesis, McMaster University.

Winchell, A. N. and Winchell, H., 1951: Elements of Optical Mineralogy; John Wiley and Sons.

Wyllie, P. J., 1960: The System CaO-MgO-FeO-SiO_2 and its Bearing on the Origin of Ultrabasic and Basic Rocks; Mineral. Mag., col. 32, 459-70.

Yoder, H. S., Jr., 1954: The System Diopside-Anorthite-Water; Carnegie Inst. Washington Yearbook 1954, 106-107.

_____ and Tilley, C. E., 1962: Origin of Basalt Magmas: An Experimental Study of Natural and Synthetic Rock Systems; J. Petr., vol. 3, 342-532.

APPENDIX

TABLE A-1. Chemical Compositions of Centre Hill Rocks Recalculated to 100 Percent, Excluding H_2O, CO_2, Ign. Numbers Prefixed by U Indicate Calculated Analyses for Respective Unit Number.

	24-05	24-10	24-13	U-3	24-18	U-5	24-23	24-25	24-28	24-33	U-10
SiO_2	47.27	45.16	50.95	46.43	42.38	51.72	42.85	51.97	43.48	50.91	43.14
TiO_2	.74	.53	.53	.47	.23	.50	.30	.46	.25	.68	.33
Al_2O_3	6.40	4.29	4.25	3.65	2.23	3.69	2.24	3.08	1.88	4.35	1.95
Fe_2O_3	3.93	7.32	1.51	3.96	11.93	1.44	11.99	1.36	12.33	1.56	12.23
FeO	10.31	6.79	8.08	6.26	5.36	7.44	5.25	6.72	5.61	9.22	5.39
MnO	.19	.19	.19	.19	.23	.18	.24	.17	.30	.20	.29
MgO	21.83	29.17	16.17	29.73	34.35	16.85	33.41	17.36	33.84	15.32	33.35
CaO	8.39	5.94	16.48	8.82	3.20	17.56	3.63	18.48	2.21	17.07	3.22
Na_2O	.76	.56	.80	.37	.05	.60	.04	.39	.04	.65	.04
K_2O	.10	.02	.03	.05	.01	.02	.01	.00	.03	.03	.03
P_2O_5	.05	.02	.01	.02	.01	.01	.02	.01	.02	.00	.02

	24-35	U-12	U-13	U-14	25-08	25-12	25-15	25-17
SiO_2	52.49	42.95	49.56	52.52	46.60	55.34	51.46	50.87
TiO_2	.84	.33	.99	1.50	1.58	1.49	1.44	1.59
Al_2O_3	5.16	1.94	10.46	13.51	14.12	13.20	13.81	13.58
Fe_2O_3	.54	12.18	4.41	3.70	3.94	3.76	3.27	2.30
FeO	9.19	5.37	13.77	13.01	15.15	12.29	11.66	13.58
MnO	.19	.28	.26	.19	.26	.24	.21	.23
MgO	13.15	33.21	9.36	3.50	7.37	2.03	5.12	6.79
CaO	16.61	3.65	8.59	8.50	7.99	5.99	8.39	7.10
Na_2O	1.68	.04	2.09	3.30	2.38	5.22	4.38	3.47
K_2O	.10	.03	.44	.18	.54	.23	.15	.39
P_2O_5	.04	.02	.06	.09	.07	.21	.09	.11

TABLE A-2. Calculation of Successive Magmas. Each Unit Width Represented as Percentage of Whole Width. Prefix U Indicates Calculated Analysis for Represented Unit. Units 10 and 12 Combined with Sample 24-28.

	27 % 25-12	15th magma	6 % 25-17	10.4% 25-15	43.4%	14th magma	6 % 25-08	49.4%	13th magma	6.4 % U-14	55.8%	12th magma
SiO_2	14.942	55.34	3.052	5.352	23.346	53.79	2.796	26.142	52.92	3.361	29.503	52.87
TiO_2	.402	1.49	.095	.150	.647	1.49	.095	.742	1.50	.096	.838	1.50
Al_2O_3	3.564	13.20	.815	1.436	5.815	13.40	.847	6.662	13.49	.865	7.527	13.49
Fe_2O_3	1.015	3.76	.138	.340	1.493	3.44	.236	1.729	3.50	.237	1.966	3.52
FeO	3.318	12.29	.815	1.213	5.346	12.32	.909	6.255	12.66	.833	7.088	12.70
MnO	.065	.24	.014	.022	.1004	.23	.016	.116	.23	.012	.128	.23
MgO	.543	2.03	.407	.533	1.488	3.43	.442	1.930	3.91	.224	2.154	3.86
CaO	1.617	5.99	.426	.873	2.916	6.72	.479	3.395	6.87	.544	3.939	7.06
Na_2O	1.409	5.22	.208	.456	2.073	4.78	.143	2.2159	4.49	.211	2.427	4.35
K_2O	.062	.23	.023	.016	.101	.23	.032	.134	.27	.012	.145	.26
P_2O_5	.057	.21	.007	.009	.073	.17	.004	.077	.16	.006	.083	.15

	8 % U-13	63.8 %	11th magma	2 % 24-35	65.8%	10th magma	8 % 24-33	73.8%	9th magma	2.4 % 24-28	76.2%	8th magma
SiO_2	3.965	33.468	52.46	1.050	34.518	52.47	4.073	38.590	52.29	1.042	39.633	52.01
TiO_2	.079	.917	1.44	.017	.934	1.42	.054	.988	1.34	.006	.995	1.31
Al_2O_3	.837	8.363	13.11	.103	8.467	12.87	.348	8.815	11.94	.045	8.860	11.63
Fe_2O_3	.353	2.319	3.63	.011	2.330	3.54	.125	2.455	3.33	.296	2.750	3.61
FeO	1.102	8.189	12.84	.184	8.373	12.73	.738	9.111	12.35	.134	9.244	12.13
MnO	.021	.149	.23	.004	.153	.23	.016	.169	.23	.007	.176	.23
MgO	.749	2.903	4.55	.263	3.166	4.81	1.226	4.392	5.95	.810	5.202	6.83
CaO	.687	4.627	7.25	.332	4.959	7.54	1.366	6.324	8.57	.057	6.381	8.37
Na_2O	.167	2.594	4.07	.034	2.628	3.99	.052	2.680	3.63	.001	2.681	3.52
K_2O	.035	.180	.28	.002	.182	.28	.002	.185	.25	.001	.185	.24
P_2O_5	.005	.088	.14	.001	.088	.13	-	.088	.12	-	.089	.12

TABLE A-2. Calculation of Successive Magmas (Continued).

	3.7 % 24-26	79.9%	7th magma	4.7 % 24-23	84.6 %	6th magma	0.7% U-5	85.3 %	5th magma	2 % 24-18	87.3 %	4th magma
SiO_2	1.923	41.556	52.01	2.014	43.570	51.54	.362	43.932	51.51	.898	44.779	51.30
TiO_2	.017	1.012	1.27	.014	1.026	1.21	.004	1.029	1.21	.005	1.034	1.18
Al_2O_3	.114	8.974	11.23	.105	9.079	10.74	.026	9.105	10.67	.045	9.150	10.48
Fe_2O_3	.050	2.801	3.51	.564	3.364	3.98	.010	3.374	3.96	.239	3.613	4.14
FeO	.249	9.493	11.88	.247	9.740	11.52	.052	9.792	11.48	.107	9.899	11.34
MnO	.006	.182	.23	.011	.194	.23	.001	.195	.23	.005	.200	.23
MgO	.642	5.844	7.31	1.57	7.414	8.77	.118	7.532	8.83	.687	8.219	9.42
CaO	.684	7.065	8.84	.171	7.236	8.56	.123	7.359	8.63	.064	7.423	8.50
Na_2O	.014	2.695	3.37	.002	2.697	3.19	.004	2.701	3.17	.001	2.702	3.10
K_2O	-	.185	.23	.001	.186	.22	-	.186	.22	-	.186	.21
P_2O_5	-	.089	.11	.001	.090	.11	-	.090	.11	-	.090	.10

	2 % U-3	89.3 %	3rd magma	6 % 24-13	95.3 %	2nd magma	4.7 % 24-08, 10	100 %	Primary magma
SiO_2	.929	45.708	51.19	3.057	48.765	51.21	2.158	50.923	50.96
TiO_2	.009	1.043	1.17	.032	1.075	1.13	.029	1.104	1.10
Al_2O_3	.073	9.223	10.33	.256	9.478	9.95	.238	9.716	9.72
Fe_2O_3	.079	3.692	4.13	.091	3.783	3.97	.286	4.069	4.07
FeO	.125	10.024	11.23	.485	10.509	11.04	.379	10.888	10.90
MnO	.004	.203	.23	.011	.215	.23	.009	.224	.22
MgO	.595	8.814	9.87	.970	9.784	10.27	1.246	11.030	11.04
CaO	.176	7.599	8.51	.989	8.588	9.02	.321	8.909	8.92
Na_2O	.007	2.710	3.03	.048	2.758	2.90	.030	2.787	2.79
K_2O	.001	.187	.21	.002	.189	.20	.002	.191	.19
P_2O_5	-	.091	.10	.001	.091	.10	.001	.093	.09

LEGEND

PRECAMBRIAN

ARCHEAN

Quartz diorite, diabase

ALGOMAN

Quartz diorite

INTRUSIVE CONTACT

BASIC AND ULTRABASIC INTRUSIVES

Gabbro (4a), gabbro (4b), peridotite (4c), pyroxenite (4d), diorite (4e), hornblende pyroxenite (4f)

INTRUSIVE CONTACT

VOLCANICS

Rhyolite, rhyolite agglomerate and tuff

Andesite, basalt

FAULTED CONTACT

SEDIMENTS

Greywacke, arkose, conglomerate (not present here)

SYMBOLS

- shrubbery or swamp
- geological boundary, defined
- geological boundary, assumed
- geological boundary, geophysical
- outcrop area
- attitude of bedding
- fault, defined
- fault, assumed
- test pit
- drill hole, horizontal projection
- sample point
- unit number

MAP 10.1

CENTRE HILL COMPLEX

TOWNSHIP OF MUNRO DISTRICT OF COCHRANE ONTARIO

Scale 1 inch = 20 feet

N.D. Macrae, 1971

(modified after Satterly, 1956)